For Reference

NOT TO BE TAKEN FROM THIS ROOM

Ex libris
Universitatis
Albertaensis

QUAECUMQUE VERA

THE UNIVERSITY OF ALBERTA

RELEASE FORM

NAME OF AUTHOR Jean Bourgois

TITLE OF THESIS Heat Transfer in a Climbing Film Evaporator

DEGREE FOR WHICH THESIS WAS PRESENTED Master of Science

YEAR THIS DEGREE GRANTED fall 1981

Permission is hereby granted to THE UNIVERSITY OF ALBERTA LIBRARY to reproduce single copies of this thesis and to lend or sell such copies for private, scholarly or scientific research purposes only.

The author reserves other publication rights, and neither the thesis nor extensive extracts from it may be printed or otherwise reproduced without the author's written permission.

THE UNIVERSITY OF ALBERTA

Heat Transfer in a Climbing Film Evaporator

by

© Jean Bourgois

A THESIS

SUBMITTED TO THE FACULTY OF GRADUATE STUDIES AND RESEARCH
IN PARTIAL FULFILMENT OF THE REQUIREMENTS FOR THE DEGREE
OF Master of Science
IN
Food Process Engineering

Department of Food Science

EDMONTON, ALBERTA
fall 1981

Digitized by the Internet Archive
in 2019 with funding from
University of Alberta Libraries

https://archive.org/details/Bourgois1981

THE UNIVERSITY OF ALBERTA

FACULTY OF GRADUATE STUDIES AND RESEARCH

The undersigned certify that they have read, and recommend to the Faculty of Graduate Studies and Research, for acceptance, a thesis entitled Heat Transfer in a Climbing Film Evaporator submitted by Jean Bourgois in partial fulfilment of the requirements for the degree of Master of Science in Food Process Engineering.

ABSTRACT

Different flow patterns are encountered in the calandria of a climbing film evaporator when the feed is introduced cold. The lower part where the feed is brought to boiling temperature is filled with liquid. The remainder of the tube where evaporation occurs contains liquid and vapor phases.

The local heat transfer coefficient and temperature profile were investigated separately for the liquid zone present in the lower part and for the boiling zone present in the upper part of a single tube glass evaporator.

A study of the heat transfer in the liquid zone, where the process liquid is brought to its boiling temperature, showed that the presence of dissolved gases affects appreciably the efficiency when the operation is carried out under vacuum as compared to an operation at atmospheric pressure.

In the boiling zone where two phase-flow is present (liquid and vapor phases), a heat transfer study permits the correlation of the pressure in the tube with the evaporating rate and the position along the evaporator tube.

A model to determine the position where boiling begins, the temperature at any position in the tube, the vapor rate and the void fraction at the exit of the evaporator tube given the initial conditions (feed rate, feed temperature, vacuum in the system and thermal properties of the feed) was set up. Its validity was demonstrated by the results obtained with sugar solutions and tomato juice. The model

was also successfully applied to an industrial scale example.

ACKNOWLEDGMENT

I would like to thank my supervisor, Dr. Marc Le Maguer, for the advice and stimulation he gave me on the research as well as the revisions to the manuscript.

I want to thank Dr. Jacob Masliyah of the Department of Chemical Engineering of the University of Alberta for his assistance with the numerical analysis.

Special thanks are due to Dr. Larry Merson of the Department of Food Science and Technology of the University of California for the data on the industrial evaporator he provided to me.

Thanks are due to Mr. Len Steele and Ms. Sara Weintraub for their assistance in the proof reading and the typing of this manuscript.

Table of Contents

Chapter Page

I. INTRODUCTION 1

II. LITERATURE REVIEW 3

A. *Climbing film and vertical tube evaporators.* ..3

B. *Two-phase flow* 5

C. *Climbing film evaporators in the food industry.* 7

1. Climbing film evaporators. 8

2. Climbing and falling film evaporators. .10

3. Plate evaporators. 10

4. Expanding flow evaporators. 11

III. EXPERIMENTAL 13

A. *Equipment.* 13

B. *Method.* 16

IV. THEORY 19

A. *Liquid zone.* 19

B. *Boiling zone.* 24

1. Pressure along the tube. 24

2. Void fraction. 30

3. Heat transfer coefficient. 31

V. RESULTS 34

A. *Liquid zone.* 34

1. Experimentation under atmospheric pressure. 34

2. Experimentation under vacuum. 40

B. *Boiling zone.* 43

VI. TESTING THE MODEL 51

A. *Distance at which boiling starts.* 51

1. No bubbles in the liquid zone. 51

2. Bubbles released in the liquid zone. ...53

B. *Temperature and vapor rate in the boiling zone.* 53

C. *Testing with liquid food.* 57

VII. DISCUSSION OF RESULTS 58

A. *Liquid zone.* 58

B. *Boiling zone.* 62

C. *About the computer programs.* 64

VIII. APPLICATION TO AN INDUSTRIAL SIZE EVAPORATOR 66

A. *Description of the evaporator.* 66

B. *Method of calculation.* 68

1. Evaluation of the amount of flashing. ..69

2. Evaluation of the heat transfer coefficient. 71

3. Results. 73

CONCLUSIONS 75

REFERENCES 77

APPENDIX A.
Data. 83

A. Temperature vs pressure for the vapor phase. 83

B. Latent heat of vaporization. 83

C. Boiling point rise of sugar solutions. .84

D. Thermal properties. 84

APPENDIX B.
Computer program for the boiling zone. 86

APPENDIX C.
Computer program for the model. 94

APPENDIX D.
Computer program for the industrial evaporator. 104

LIST OF TABLES

Table Description....................Page

1 Coefficients A, B and C from equation 44............38

2 Temperature profiles in the boiling zone for seven different feed rates. The steam pressure and the vacuum remain the same.........................46

3 Temperature profiles in the boiling zone for different steam pressures. The vacuum and the feed rate remain the same..............................47

4 Temperature profiles in the boiling zone for different vacuums. The steam pressure and the feed rate remain the same..............................48

5 Mean and standard deviation of the heat transfer coefficient in the boiling zone..................49

6 Comparison between experimental values and values predicted by the model for tap water.........55

7 Comparison between experimental values and values predicted by the model for degassed water and different liquid solutions................56

8 Computed values for the industrial evaporator.......74

LIST OF FIGURES

Figure..page

1 Schematic diagram of the evaporator.................14

2 Cross section of the evaporator tube in the liquid zone...................................20

3 Cross section of the evaporator tube in the boiling zone..................................32

4 Temperature profile in the liquid zone..............35

5 Liquid zone: ln of the dimensionless temperature T^* vs the dimensionless position Z^*..................37

6 Coefficients A, B and C from equation 44 vs $1/Pe_l$ .The curves represent the best least squares fit....................................39

7 Comparison between temperature profiles in the liquid zone for tap water and degassed water. The flow rates are identical.................41

8 Temperature profile in the boiling zone.............45

9 Best least squares fit of the heat transfer coefficient in the boiling zone.......................50

10 Temperature profiles in the liquid zone as a combination of laminar flow and natural convection flow...................................60

11 Schematic diagram of the industrial evaporator......67

LIST OF SYMBOLS

Cp	Heat capacity	$J.kg^{-1}.K^{-1}$
D	Inside diameter of the calandria	m
F	Friction term	$N.m^{-3}$
G	Mass flux	$kg.m^{-2}.s^{-1}$
g	Acceleration of gravity	$m.s^{-2}$
gr	Gravity term	$N.m^{-3}$
j	Volumetric flux	$m.s^{-1}$
k	Thermal conductivity	$W.m^{-1}.K^{-1}$
L	Tube length	m
P	Pressure	Pa
R	Gas Constant for vapor phase	$J.kg^{-1}.K^{-1}$
S	Slip ratio: $S = V_2/V_1$	
T	Temperature	°C or K
U	Heat transfer coefficient	$W.m^{-2}.K^{-1}$
V	Velocity	$m.s^{-1}$
W	Mass flow rate	$kg.s^{-1}$
z	Position in the tube	m
α	Void fraction of the vapor	
ψ	Evaporation rate of water	$kg.m^{-3}.s^{-1}$
λ	Enthalpy of vaporisation	$J.kg^{-1}$
μ	Viscosity	$kg.m^{-1}.s^{-1}$
ρ	Density	$kg.m^{-3}$

Subscripts

A	Glass evaporator
B	Industrial evaporator
b	Where boiling begins
f	In the climbing film
i	Inlet conditions
ln	Logarithmic mean
v	Vapor
s	Steam
z	At position z (local)
1	Liquid phase
2	Vapor phase

Dimensionless groups

$Nu_z = U_z.L/k_i$	Nusselt Number.
$Re = 4.W/\pi.\mu.D$	Reynolds Number.
$Pr = \mu.Cp/k$	Prandtl Number.
$Pe = Re.Pr$	Peclet Number.
$j_1* = j_1\sqrt{\rho_1}/\sqrt{g.D(\rho_1 - \rho_2)}$	Dimensionless volumetric flux.
$j_2* = j_2\sqrt{\rho_2}/\sqrt{g.D(\rho_1 - \rho_2)}$	Dimensionless volumetric flux.
$T* = (T_s - T_i)/(T_s - T)$	Dimensionless temperature.
$Z* = z/L$	Dimensionless length.

I. INTRODUCTION

The concentration of solutions by evaporation of part of the solvent is a very common practice in the chemical, pharmaceutical and food processing industries. When the material being handled is heat sensitive, the problem is made more complicated by the need to avoid exposure of the material to high temperatures or a long contact time with the heating surface.

The use of a climbing film evaporator is often the best solution, as high rates of heat transfer can be maintained without the use of high temperatures or long contact time.

Since 1899, when it was introduced by Paul Kestner, the climbing film evaporator has been used to a continually increasing extent in the chemical and food industries. Besides the short time of contact and the low temperature, the small hold up and relatively simple construction are among its prime advantages. Its use is not confined to the concentration of aqueous liquors, the same form of unit is also employed as a reboiler on fractionating columns. Although of a different conception, the exchangers used for decompression in water cooled nuclear reactors show a similar flow pattern in the tubes.

Despite its industrial importance, there are relatively few papers in the literature in which precise performance details are available, and the climbing film evaporators are designed largely from experience and not from any established relationship between the operating conditions,

the physical properties of the liquor and the consequent heat flux or transfer coefficient.

This research was carried out to fill this gap by establishing relations to define a model which enables one to determine the performance of the evaporator by control of the different parameters present in the system.

In this research a borosilicate glass climbing film evaporator was used. The influence of the operating factors on the local heat transfer and temperature profile in the liquid zone as well as in the boiling zone is described and discussed together with the influence of these same parameters on the distance at which boiling starts in the tube.

The proposed model is validated with the results obtained with water and is successfully tested with sugar solutions and tomato juice.

The model developed for the single tube glass evaporator was tested on an industrial evaporator made of three sections, the first one having 66 tubes, the second 111 tubes and the third 156 tubes and capable of concentrating 5,000 kg per hour of pineapple juice from 13.5°Brix to 62°Brix.

II. LITERATURE REVIEW

A. *Climbing film and vertical tube evaporators.*

A review covering the period 1970 to 1980 shows that little work had been done recently in this area.

The research on vertical tube evaporators was generally conducted in desalination or wastewater plants. Multiple effect vertical tube evaporators in desalination plants with a capacity of up to 500 tons per day were described and their performance under different conditions analysed.

Sephton *et al.* (1973) and Sephton (1975, 1976) showed that the addition of surfactant in sea water or wastewater permits a more stable operation and an increase in the heat transfer coefficient up to 100% with a differential temperature 2°C lower. They also demonstrated the superiority of upflow vertical tube evaporators versus downflow vertical tube evaporators.

Gel'Perin *et al.* (1973) studied the overall heat transfer coefficient for boiling mixtures of organic liquids in a vertical tube evaporator. They developed an empirical equation to evaluate the overall heat transfer coefficient in boiling aqueous inorganic salt solutions as a function of the heat flux, the concentration and the apparent liquid level in a thermosiphon evaporator.

Takeda *et al.* (1972, 1973) studied the effect of vapor hold up on the boiling heat transfer coefficient in a natural circulation vertical tube evaporator, but once

again, no attempt was made to determine the local heat transfer coefficient and the overall heat transfer coefficient did not take into account the different zones encountered in a vertical tube evaporator (liquid not boiling at the bottom and two phase flow in the upper part).

Arellano Gajardo (1972) used an apparatus similar to ours (pyrex glass climbing film evaporator) to determine the chemical, nutritive and organoleptic changes in concentration of milk, orange juice and grape juice. He only made a mass balance study to determine the evaporative efficiency of the climbilng film evaporator.

In previous works covering the period 1945 - 1970, some authors noticed that the successive flow patterns encountered in the tube made difficult the determination of the heat transfer coefficient because the ratio of the non-boiling zone length to the boiling zone length in the tube was a function of the feed temperature, feed rate and of all the other variables in the system. The calculated overall heat transfer coefficient differed from one experiment to another. To avoid this problem, Coulson and McNelly (1956) introduced the feed at boiling temperature. They found three different forms of heat transfer along the tube depending on the feed rate and the differential temperature between the heating media and the product. While using a traveling thermocouple to measure the temperature in the tube, they did not explore the full capacity of their apparatus and kept calculating overall heat transfer

coefficients based on the average temperature in the tube.

Guerrieri and Talty (1956) installed thermocouples every 6 inches in a 6 feet long vertical tube evaporator and studied the local heat transfer to organic liquids, but unfortunately they developed their study from the Lockhart and Martinelli (1949) pressure drop correlation for two-phase flow. This correlation was developed for isothermal two-phase, two-component flow in pipes without phase change, which does not correspond to the experimental conditions encountered by Guerrieri and Talty.

B. *Two-phase flow*

A literature review on two-phase flow shows that the prediction of heat and mass transfer when a liquid phase and a gaseous phase are present in a tube is difficult because of the number of parameters involved. The present knowledge of heat transfer in such flow systems is limited and results obtained for one set of conditions are of little value in predicting performance at a different set of conditions.

Lunde (1961) tried to find a correlation for two-phase, two-component heat transfer on the basis of a physical model. He took the data obtained by different authors and correlated them for the supposed different flow patterns encountered (stratified flow, slug flow, annular flow); in most cases the deviation of the experimental data from the proposed correlation is up to 30%. Sometimes points are outside the 30% deviation zone. This model permits only the

evaluation of an overall heat transfer coefficient. This model is probably acceptable when the change of phase in the exchanger is kept at a minimum to ensure that the ratio of gas to liquid does not vary too much and that the assumed flow pattern stays the same all along the tube, which is not the case in our study.

Lunde (1961) showed in his study that the critical Reynolds Number for the transition between viscous and turbulent regions is smaller for two-phase flow than for one-phase flow. This phenomenon was confirmed by Kao *et al.* (1972) in their analysis of the stability of film boiling on vertical surfaces.

A complete analysis of one-dimensional two-phase flow was made by Wallis (1969). A review of all the possible problems encountered in one-dimensional two-phase flow was given and equations proposed by different authors were discussed. When no phase change occurs in the tube, the validity of the proposed equations which are based on continuity and momentum is without equivocation; but when it comes to flow with phase change, the different authors do not agree on the repartition of the force for momentum increase due to phase change per unit volume between the liquid phase and the vapor phase. This repartition appears to be function of the process, the hydrodynamic mechanism and the rate of vaporisation.

Malnes (1975), in his analysis of critical two-phase flow based on non-equilibrium effects, showed that in real

systems, two-dimensional effects occur and affect the values predicted by a one-dimensional theory by an increase of the exit pressure and a decrease of exit velocities. To obtain results in accordance with reality, Malnes (1975) had to introduce a correlation for the slip ratio between the vapor phase and the liquid phase and a correlation for flashing occuring along the tube of the evaporator.

C. *Climbing film evaporators in the food industry.*

In food processing, evaporation implies a unit operation where the concentration of a solution is increased by driving off a portion of the solvent in the form of vapor. In most cases the solvent vaporised is water and the concentrated solution is the desired product.

The problem is far more complex than the evaporation of most chemical products, as the end product is not only subject to physical and biological testing but to organoleptic analysis. Such hard-to-define parameters as taste, odor, color and texture must be of prime concern in the process design as well as in the equipment design and operation.

It is essential that the evaporation of water from the product by heat shall be mild enough to preserve the nutritive value of the product and prevent browning reactions, either by caramelisation of sugars or by reaction between protein and sugars. Also, undue denaturation of the proteins and destruction of vitamins by excess or prolonged

heating is undesirable.

The oldest of the evaporators is the shell and tube type. The first real advancement in evaporating equipment was made in 1813 when E. C. Howard invented the vacuum pan which reduced the boiling temperature by about one-half. As stated earlier, the next major step occurred in 1899 when P. Kestner invented the vertical tube climbing film evaporator.

Unfortunatly, the climbing film evaporator as a unit has not found much favour in the food industry. Many evaporators, if not classified as true climbing film, contain a section where climbing film evaporation is encountered. It is useful to review these evaporators and their use in the food industry.

1. Climbing film evaporators.

Sometimes it is necessary to produce from a very weak liquor a highly concentrated finish product. A single pass climbing film evaporator will not solve this problem. One solution is to recirculate the liquor through the evaporator. Another solution is to pass the liquor in series through two or more evaporator units. This is known as the multi-circulation climbing film evaporator (Slade, 1967).

It includes two or more calandrias. These calandrias are formed by dividing a simple steam shell into two or more sections of tubes, each section having fewer tubes than the preceding one and being provided with a separator at the top. The flow of liquor passing through each section and

each separator in series progressively diminishes in quantity, but since the number of tubes is progressively reduced, an adequate flow is provided in each section to maintain a climbing film condition. Such an evaporator has been used for handling heat sensitive liquors such as coffee, fruit juices, milk, tea, whey and wine.

The calandria short vertical tube evaporator as described by Moore and Hesler (1963) has been used for over a century in the sugar industry but cannot be considered as a true climbing film evaporator, the tubes being too short to obtain a true film boiling zone.

The sloping calandria evaporator described by Brennan *et al.* (1969) looks like a recirculating climbing film evaporator tilted in an inclined position. It was widely used in the dairy industry up to the mid-fifties when it was progressively replaced by more sophisticated evaporators (Scott, 1964).

Liquid food-stuffs very sensitive to heat can be evaporated at very low temperature in a low temperature evaporator (Slade, 1967). Such an evaporator is of the recirculating climbing film type and is used under high vacuum. The boiling point of the liquor being of the order of 15°C, the temperature of the condenser water usually available for other types of evaporators is too high to condense the vapor formed at such a low pressure; this is why an auxiliary fluid (ammonia) is used. It works on the principle of the heat pump; the heating fluid is vaporized

to cool the condenser, then recompressed through a compressor to supply heat to the calandria.

The low temperature evaporator was widely used in the concentration of orange juice following the Second World War but was replaced by single pass evaporators, where the advantage of the low temperature was overcome by the decrease in residence time leading to similar or even better organoleptic qualities of the concentrated juice.

2. Climbing and falling film evaporators.

A combination of the climbing and falling film may be used where a high percentage of evaporation is required and when the concentrated liquor tends to be viscous; as the most concentrated liquor is formed in the falling film section, the flow is improved by the gravity force. It is generally used as a finisher evaporator following a climbing film evaporator where the greatest part of the evaporation has been effected. It has been used to produce orange and tomato juices.

3. Plate evaporators.

The plate evaporator is well described by Carter and Kraybill (1966). It differs from the conventional evaporator in that the tubular calandria is replaced by a series of plates. The plates are arranged so that the liquid passes through a rising film section, then down through a falling film section with each product plate sandwiched between two steam plates. A very high surface to volume ratio is achieved, thereby reducing the holdup time.

Sanitary type stainless-steel centrifugal pumps are generally employed for liquor feed, and a velocity up to 80 $m.s^{-1}$ can be achieved in the last plates of the evaporator (Papadopoulos and Samuel, 1965).

Among the other advantages of the plate evaporator are its compactness, the possibility of increasing the capacity rapidly by adding plates and the good access for cleaning by quick disconnection of the plates. A further obvious advantage is that should any plate failure occur, a replacement can be made immediately with a minimum loss of production time.

Lawler (1960) and Papadopoulos and Samuel (1965) discuss the use of this evaporator in the concentration of orange juice and beer wort. It is widely in use all over the world to concentrate a great variety of products such as skim milk, whole milk, buttermilk, whey, ice cream mix, apple juice, orange juice, pear juice, lemon juices, apple pectin, chicken broth, gelatin, jam and table jelly.

4. Expanding flow evaporators.

This type of evaporator is almost exclusively used in the dairy industry. It is well described by Brennan *et al.* (1969). In this device milk and steam flow through alternate passages in a manner similar to that in a plate evaporator. The plates are replaced by thin, inverted stainless steel cones, gasketed to prevent leakage. Milk enters through a central spindle at the base of the cone assembly and is fed, via nozzles, to the heated cone spaces.

Flowing upwards and outwards over the steam-heated surfaces, under vacuum conditions the milk rapidly attains its boiling point. A high velocity vapour-liquid stream leaves the cone assembly tangentially, ensuring a good separation.

III. EXPERIMENTAL

A. *Equipment.*

The evaporator is a Q.V.F. CFE1 climbing film evaporator made of borosilicate glass. A schematic diagram of the evaporator is presented in Figure 1.

It is composed of three parts:

1. The evaporator part which is made of a calandria tube 3m long, 3cm inside diameter and 1.53mm wall thickness. This calandria is enclosed in a steam jacket made of a 2.70m long, 5cm bore glass pipe which can withstand steam pressure of 3 bars absolute. It has three branches for steam inlet, condensed steam and vent connections.
2. The inside evaporator tube leads from the calandria to the condenser via a cyclone separator which separates the entrained liquid from the vapor. The liquid outlet of the separator is connected directly to the concentrate receiver. The separator and the concentrate receiver form the second part of the apparatus.
3. The third part of the evaporator is composed of the vapor condenser directly connected to the vapor exit of the cyclone separator. The bottom part of the condenser leads to two 5 liters condensate receivers.

Each condensate receiver is connected to the vacuum line. The two receivers are separated by a valve to enable the condensate to be removed during the operation of the evaporator. When the lower one is full of condensed water,

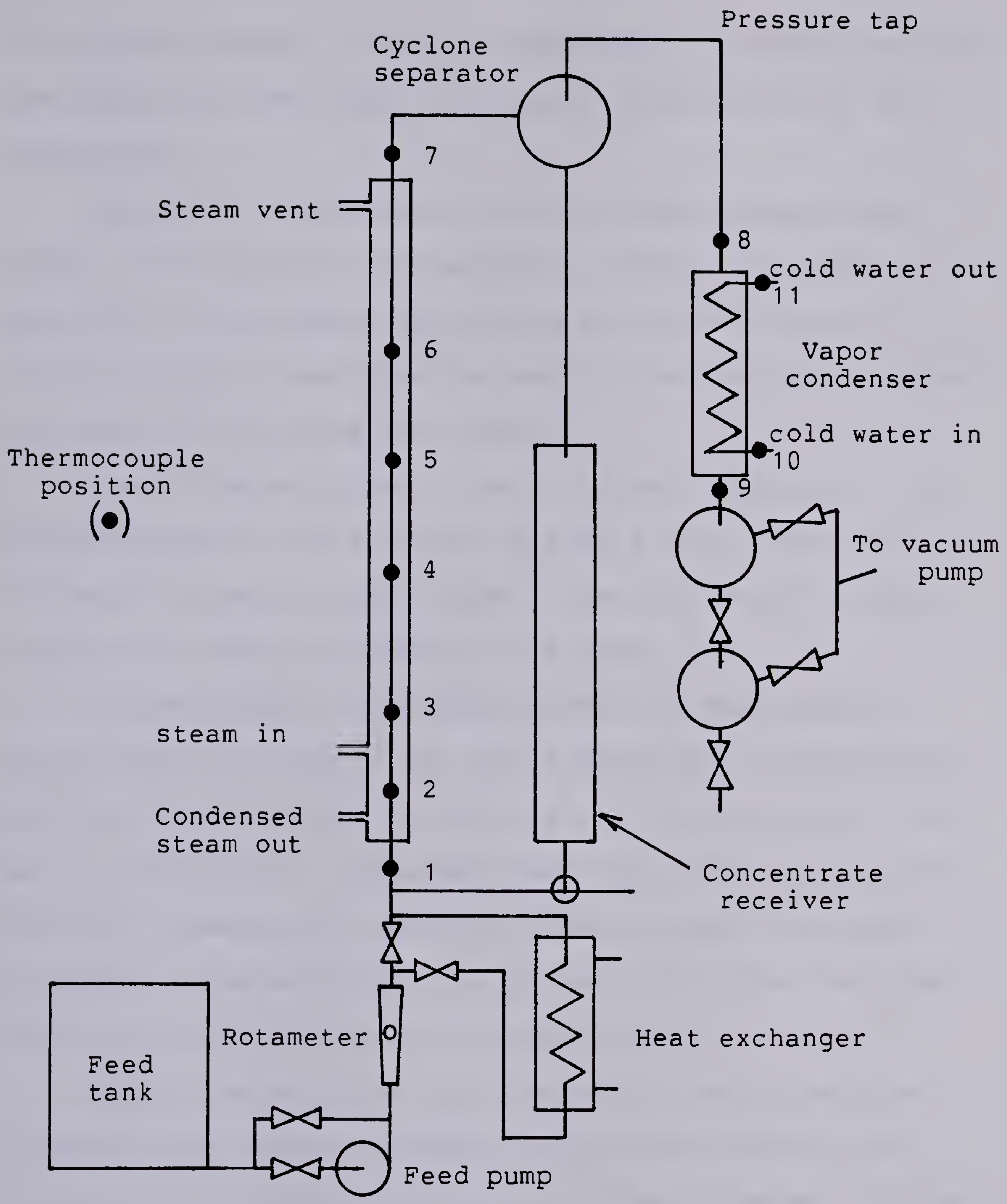
Pressure tap
Cyclone separator
7
Steam vent
8
cold water out
11
Vapor condenser
6
cold water in
10
Thermocouple position
(●)
5
9
4
To vacuum pump
3
steam in
2
Condensed steam out
1
Concentrate receiver
Rotameter
Heat exchanger
Feed tank
Feed pump

Fig. 1. Schematic diagram of the evaporator.

it can be isolated, vented to atmospheric pressure, emptied and vacuum can be reapplied without interruption of the experiment.

The unit is connected to a Nash Hytor vacuum pump model 673 capable of maintaining a pressure of 160mm of mercury in the system. The vacuum can be adjusted for operation and released at the end of the operation by means of a vent cock on the main line.

Seven thermocouples, type T (copper constantan), are placed along the axis of the calandria tube. The wires are 0.46mm in diameter and a common constantan wire is used to reduce the number of wires in the tube.

Thermocouple 1 is located under the steam jacket connection and records the feed temperature. Thermocouples 2, 3, 4, 5 and 6 are located at 0.15m, 0.45m, 0.95m, 1.45m and 1.95m from the condensed steam vent which is taken as origin to measure the position along the heat exchanger calandria. Thermocouple 7 is located just above the steam jacket and records the exit temperature.

Other thermocouples are located on the top and the bottom of the vapor condenser, at the inlet and at the outlet of the cooling water line of the condenser. Another thermocouple is kept in a bath of ice in water and is used as reference to zero the recorder.

The twelve thermocouples are connected to a twelve point multipoint recorder (Honeywell Electronik model 112) calibrated in degrees centigrade with a range 0 to 100°C.

A pressure tap located between the cyclone separator and the vapor condenser is connected to a mercury manometer to obtain an accurate reading of the vacuum in the system.

The steam is supplied through a variable pressure control valve which adjusts the steam pressure to the desired value. The feed rate, when using a clear solution, is measured through a set of two rotameters with a maximum capacity of 3kg/min of water at 20°C.

B. *Method.*

In normal use of the evaporator, different zones are present in the calandria tube (liquid zone at the lower part and film boiling zone at the upper part). Because in each zone the heat transfer is controlled by a different mechanism, the study was divided into three parts:

1. Experimentation with the liquid phase filling completely the tube with no evaporation. The evaporator is used as a single tube heat exchanger. This gives the correlation of the local heat transfer in the liquid zone.
2. Experimentation with the liquid entering the evaporator at its boiling temperature to obtain a two-phase flow pattern all along the tube and develop a model for the climbing film ebullition zone.
3. In the third part, a model is proposed which by combination of the relationships obtained in the two previous sections permits the prediction of the performance of the evaporator in normal use (distance at

which boiling starts, vapor rate at the exit and temperature profile along the tube) knowing the inlet conditions.

The correlations governing the liquid zone were determined from data obtained using water as a medium. In this section, the evaporator was run at atmospheric pressure and the water was fed by means of a variable flow positive pressure pump. The lower flow rate is limited by the water reaching boiling temperature at the exit of the evaporator tube while the maximum rate is limited by the capacity of the rotameter.

Correlations in the film boiling zone were determined using water as medium. The evaporator was run under controlled vacuum and the feed temperature was adjusted to the boiling temperature corresponding to the pressure in the system by means of an heat exchanger mounted prior to the evaporator inlet.

The feed is introduced under a pressure gradient existing between the container, where it is stored at atmospheric pressure, and the vacuum in the system. The rate is controlled by means of a needle valve placed on the feed line.

The validity of the model developed in the third part was tested using water, sucrose solutions of different concentration and commercial tomato juice.

A typical run with the evaporator is as follows:

1. The steam pressure, vacuum and feed rate are set at the

desired values.

2. After a few minutes when a steady state has been reached (the temperature profile along the tube does not change any more), the level of concentrate in the concentrate receiver is noted and the time is set at zero.
3. When either the concentrate receiver or the condensate receiver are almost full, the level in the concentrate receiver is recorded again at time t. The concentrate receiver having been calibrated, the rate of concentrate collection is evaluated.
4. The rate of vapor formation at the exit of the evaporator is obtained by difference between the feed rate and the concentrate rate.

IV. THEORY

A. *Liquid zone.*

When there is only the liquid phase present in the tube, considering a tube section of length dz, the heat flow from the steam to the liquid can be evaluated as follows (refer to Figure 2):

$$q = W.Cp.dT = U_z.dA.(T_s - T) \tag{1}$$

$$\text{with } dA = \pi.D.dz \tag{2}$$

Solving for U_z we obtain:

$$U_z.dz = \frac{W.Cp}{\pi.D} \frac{dT}{(T_s - T)} \tag{3}$$

Dimensionalization of the equations:

$$Z* = \frac{z}{L} \qquad dZ* = \frac{dz}{L} \tag{4}$$

$$T* = \frac{(T_s - T_i)}{(T_s - T)} \qquad dT* = \frac{(T_s - T_i)}{(T_s - T)^2} dT \tag{5}$$

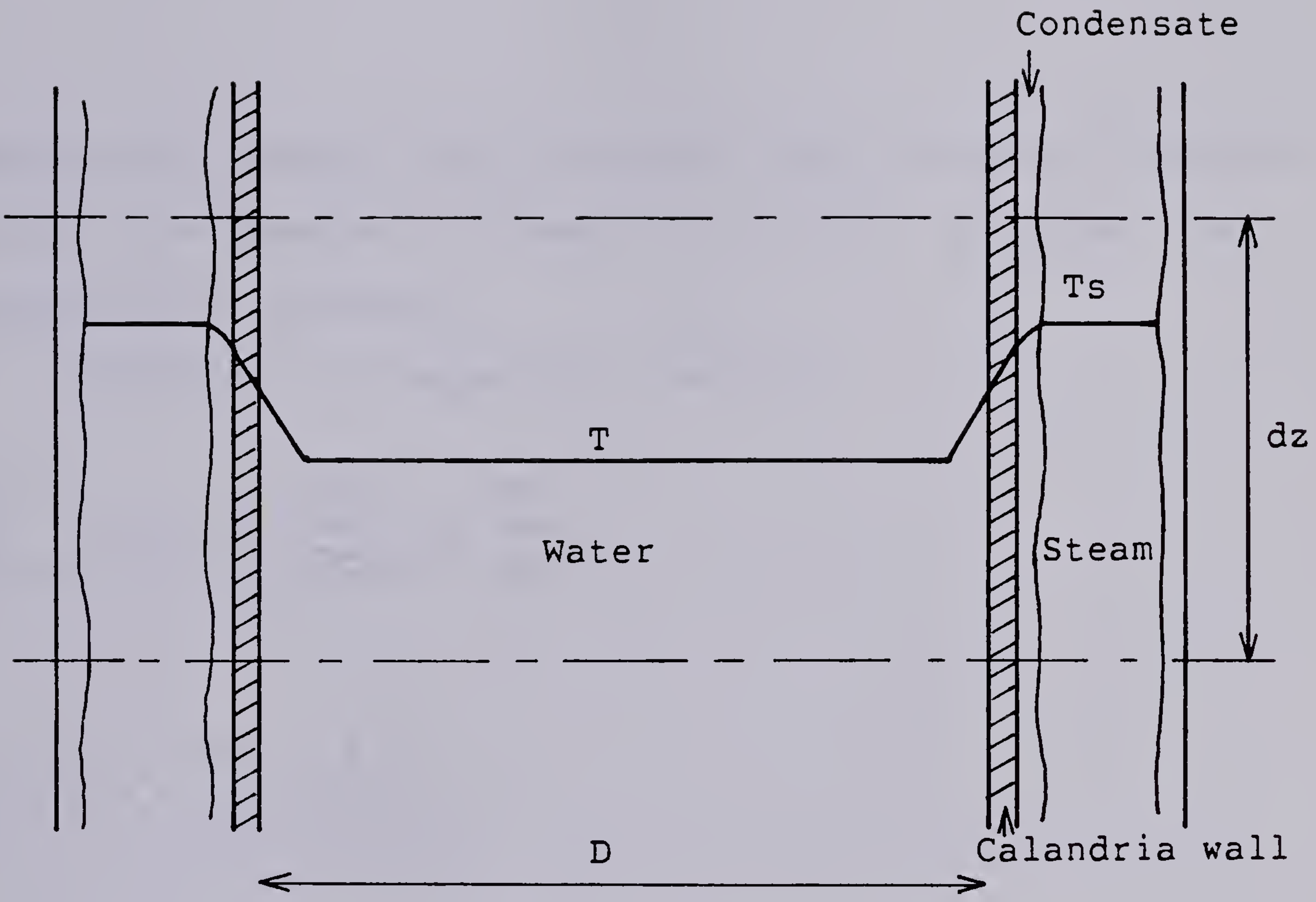
Condensate
Ts
T
dz
Water
Steam
D
Calandria wall

Fig. 2. Cross section of the evaporator tube in the liquid zone.

Equation 3 becomes:

$$U_z . dZ* = \frac{W.Cp}{\pi.D.L} \frac{dT*}{T*} \qquad (6)$$

Because the specific heat of liquid food varies by less than 1% over the temperature range 0°C to 100°C, we assume that $W.Cp/\pi.D.L$ is constant.

Integration of Equation 6 leads to:

$$\int_{Z_o*}^{Z*} U_z . dZ* = \frac{W.Cp}{\pi.D.L} \ln \frac{T*}{T_o*}$$

$$\text{with } T_o* = \frac{(T_s - T_i)}{(T_s - T_i)} = 1$$

$$\int_{Z_o*}^{Z*} U_z . dZ* = \frac{W.Cp}{\pi.D.L} \ln(T*) \qquad (7)$$

For a given flow rate and a known initial temperature, ln(T*) is only a function of the position Z* in the tube.

Equation 6 can be rewritten as:

$$U_z = \frac{W.Cp}{\pi.D.L} \frac{d\ln(T*)}{dZ*} \tag{8}$$

Let us introduce the Peclet Number which is the product of the Reynolds Number by the Prandlt Number.

$$Re = \frac{4.W}{\pi.\mu.D} \quad \text{and} \quad Pr = \frac{\mu.Cp}{k}$$

$$Pe = Re.Pr = \frac{4.W.Cp}{\pi.D.k} \tag{9}$$

The initial Peclet Number (at the inlet of the evaporator tube) is defined as follows:

$$Pe_i = \frac{4.W.Cp}{\pi.D.k_i} \tag{10}$$

Equation 8 becomes:

$$U_z = \frac{Pe_i}{4.L}.k_i \frac{d\ln(T*)}{dZ*} \tag{11}$$

Rearrangement of Equation 11 leads to:

$$\frac{U_z.L}{k_i} = \frac{Pe_i}{4}\frac{d\ln(T*)}{dZ*}$$

$U_z.L/k_i$ can be defined as a local Nusselt Number (Nu_z) characteristic of our evaporator length and overall heat transfer coefficient at position z.

Equation 11 becomes:

$$Nu_z = \frac{Pe_i}{4}\frac{d\ln(T*)}{dZ*} \tag{12}$$

With ln(T*) only a function of Z* and Pe_i. Therefore the heat transfer in the liquid zone should follow an equation of the form:

$$Nu_z = f(Pe_i, Z*) \tag{13}$$

This relation is to be determined empirically from experimental data. This will be done in the Results Section. When Equation 13 is known, it will be used to predict the temperature in the liquid zone using Equation 7.

B. *Boiling zone.*

1. Pressure along the tube.

We assume that the vapor phase is always saturated.

Using the equations proposed by Malnes (1975) we define the continuity and momentum equations as follows:

Continuity:

$$\frac{dG_1}{dz} = -\psi \qquad (14)$$

$$\frac{dG_2}{dz} = \psi \qquad (15)$$

Momentum:

$$0 = \frac{dP}{dz} - \frac{d}{dz}(G_1.V_1 + G_2.V_2) - F - gr \qquad (16)$$

where

F = Friction term.

gr = Gravity head.

We define the slip ratio as follow:

$$S = \frac{V_2}{V_1} \tag{17}$$

Therefore we have, assuming that S stays constant (refer to the Discussion of Results Section):

$$\frac{dV_2}{dz} = S \frac{dV_1}{dz} \tag{18}$$

Levy (1960) suggested that, if evaporation is rapid enough (which is the case in our study), inertia and phase change terms are usually much larger than friction and body terms. So we assume F = 0 and Equation 16 becomes:

$$\frac{dP}{dz} + V_1 \frac{dG_1}{dz} + G_1 \frac{dV_1}{dz} + V_2 \frac{dG_2}{dz} + G_2 \frac{dV_2}{dz} + gr = 0 \tag{19}$$

The mass fluxes are defined as follows:

$$G_1 = \rho_1 . V_1 (1 - \alpha) \tag{20}$$

$$G_2 = \rho_2 . V_2 . \alpha \tag{21}$$

Development of Equations 14 to 21 leads to:

$$\frac{dP}{dz} - \psi . V_1 + \rho_1 . V_1 (1 - \alpha) \frac{dV_1}{dz} + S . V_1 . \psi + \rho_2 . S^2 . V_1 . \alpha \frac{dV_1}{dz} + gr = 0 \qquad (22)$$

Differentiation of Equations 20 and 21 with respect to z gives, respectively:

$$\frac{dG_1}{dz} = -\psi = (1 - \alpha) . (\rho_1 \frac{dV_1}{dz} + V_1 \frac{d\rho_1}{dz}) - \rho_1 . V_1 \frac{d\alpha}{dz} \qquad (23)$$

and

$$\frac{dG_2}{dz} = \psi = S . \alpha . (\rho_2 \frac{dV_1}{dz} + V_1 \frac{d\rho_2}{dz}) + S . \rho_2 . V_1 \frac{d\alpha}{dz} \qquad (24)$$

Elimination of $d\alpha/dz$ between Equations 23 and 24 and solving for dV_1/dz gives:

$$\frac{dV_1}{dz} = \psi \frac{(\rho_1 - S . \rho_2)}{S . \rho_1 . \rho_2} - V_1 (\frac{\alpha}{\rho_2} \frac{d\rho_2}{dz} + \frac{(1 - \alpha)}{\rho_1} \frac{d\rho_1}{dz}) \qquad (25)$$

Equations 22 and 25 give:

$$\frac{dP}{dz}+V_1.\psi.(\rho\frac{(\rho_1 - S.\rho_2)}{S.\rho_1.\rho_2}+S-1)-\rho.V_1^2(\frac{\alpha}{\rho_2}\frac{d\rho_2}{dz}+\frac{(1-\alpha)}{\rho_1}\frac{d\rho_1}{dz})+gr=0 \qquad (26)$$

with $\rho = \alpha.\rho_2.S^2 + (1 - \alpha)\rho_1$ (27)

$d\rho_1/dz$ and $d\rho_2/dz$ are as follows:

$$\frac{d\rho_1}{dz} = \frac{\partial\rho_1}{\partial T}\frac{\partial T}{\partial z} + \frac{\partial\rho_1}{\partial P}\frac{\partial P}{\partial z}$$

$$\frac{d\rho_2}{dz} = \frac{\partial\rho_2}{\partial P}\frac{\partial P}{\partial z} + \frac{\partial\rho_2}{\partial T}\frac{\partial T}{\partial z}$$

Because the liquid phase is incompressible we have: $\partial\rho_1/\partial P=0$. The temperature does not vary too much in the boiling zone and $\partial\rho_1/\partial T.\partial T/\partial z$ can be neglected, so we assume $d\rho_1/dz=0$.

The temperature of saturated vapor is only a function of the pressure; therefore ρ_2 is only a function of the pressure.

We have now:

$$\frac{d\rho_1}{dz} = 0 \tag{28}$$

$$\frac{d\rho_2}{dz} = \frac{\partial\rho_2}{\partial P}\,\frac{dP}{dz} \tag{29}$$

Introduction of Equation 29 in Equation 26 gives:

$$\frac{dP}{dz}\left(1 - \rho.V_1{}^2\,\frac{\alpha}{\rho_2}\,\frac{\partial\rho_2}{\partial P}\right) = -\,V_1.\psi\left(\rho\frac{(\rho_1 - S.\rho_2)}{S.\rho_1.\rho_2} + S-1\right) - gr \tag{30}$$

Along the saturation curve of water the absolute temperature and the pressure can be correlated by:

$$\begin{array}{lcl} T = c.P^n & & \\ T\ (K) & \text{with} & \left\{\begin{array}{l} c = 166.766 \\ \quad\text{and} \\ n = 0.06978 \end{array}\right. \\ P\ (Pa) & & \end{array} \tag{31}$$

For ideal gases we have:

$$P = \rho_2.R.T \tag{32}$$

where R is the gas constant defined as follows:

$R = \mathrm{R}/\mathrm{M}$ where M is the molecular weight and R is the universal gas constant and is equal to 8314.5 $\mathrm{J.kmole^{-1}.K^{-1}}$

then $P = \rho_2.R.c.P^n \quad \rightarrow \quad \rho_2 = (1/R.c).P^{1-n}$

$$\frac{\partial \rho_2}{\partial P} = \frac{1-n}{R.c} P^{-n} \qquad (33)$$

The gravity head is defined as follows:

$$gr = g.(\alpha.\rho_2 + \rho_1(1-\alpha)) \qquad (34)$$

Equation 30 becomes:

$$\frac{dP}{dz} = \frac{-V_1.\psi(\rho \dfrac{(\rho_1 - S.\rho_2)}{S.\rho_1.\rho_2} + S - 1) - g.(\alpha.\rho_2 + \rho_1(1-\alpha))}{1 - \rho.V_1{}^2 \dfrac{\alpha}{\rho_2} \dfrac{(1-n)}{R.c} P^{-n}} \qquad (35)$$

Let us introduce the dimensionless length Z* and the rate of evaporation of water per unit volume:

$$\psi = \frac{dW_2}{\pi . R^2 . L . dZ*} \qquad (36)$$

Introduction of Equation 36 in Equation 35 gives:

$$\frac{dP}{dZ*} = \frac{- \frac{V_1}{\pi . R^2} \left(\rho \frac{(\rho_1 - S . \rho_2)}{S . \rho_1 . \rho_2} + S - 1 \right) \frac{dW_2}{dZ*} - g . (\alpha . \rho_2 + \rho_1 (1 - \alpha)) L}{1 - \rho . V_1{}^2 \frac{\alpha}{\rho_2} \frac{(1 - n)}{R . c} P^{-n}} \qquad (37)$$

The pressure can be obtained in the boiling zone by solving Equation 37 if $dW_2/dZ*$ and α are known.

2. Void fraction.

α is not known but it can be estimated with the modified Darmouth correlation for vertical upward cocurrent annular flow as proposed by Turner (1966):

$$\frac{j_2*}{1 - 3.1 (1 - \alpha)} - \frac{j_1*}{3.1 (1 - \alpha)} = 1 \qquad (38)$$

Where j_1* and j_2* are the dimensionless volumetric fluxes defined below.

$$j_1* = \frac{j_1 \sqrt{\rho_1}}{\sqrt{g . D (\rho_1 - \rho_2)}} \qquad \text{and} \qquad j_2* = \frac{j_2 \sqrt{\rho_2}}{\sqrt{g . D (\rho_1 - \rho_2)}}$$

3. Heat transfer coefficient.

The heat balance at position z is defined as follows (refer to Figure 3):

$$q = U_z.\pi.D.dz\ (T_s - T) = \lambda.dW_2 + (W_1.Cp_1 + W_2.Cp_2).dT \qquad (39)$$

T is the temperature of the liquid at the interphase. It is slightly higher than the vapor temperature due to the effect of the boiling point rise for solutions other than pure water.

Equation 39 leads to:

$$U_z.\pi.D(T_s - T) = \lambda \frac{dW_2}{dz} + (W_1.Cp_1 + W_2.Cp_2) \frac{dT}{dz} \qquad (40)$$

Introduction of the dimensionless length gives:

$$U_z.\pi.D.L(T_s - T) = \lambda \frac{dW_2}{dZ*} + (W_1.Cp_1 + W_2.Cp_2) \frac{dT}{dP} \frac{dP}{dZ*} \qquad (41)$$

Recall Equation 31:

$T_s = c.P_s^n$ and $T = c.P^n$

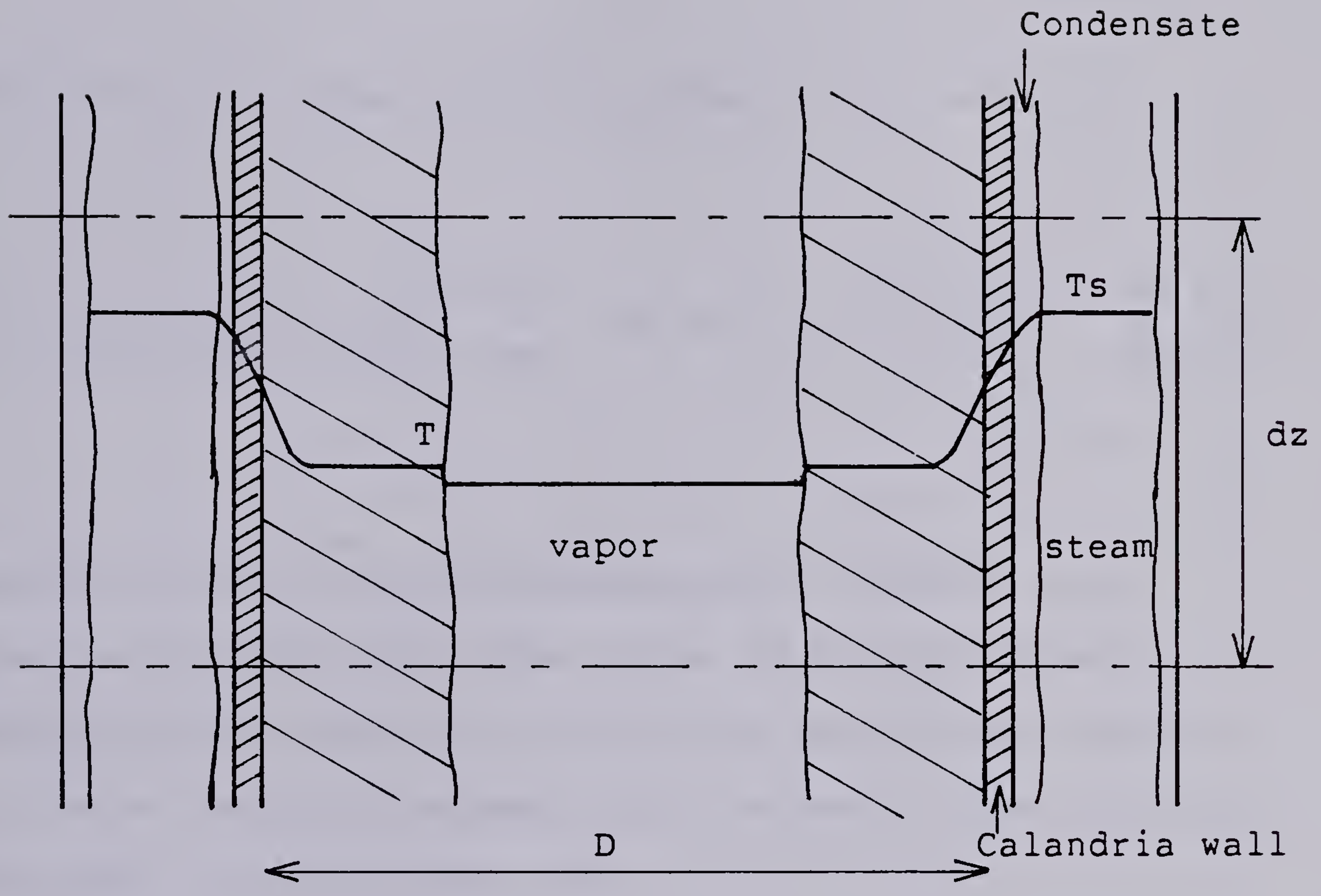
Condensate
Ts
T
dz
vapor
steam
D
Calandria wall

Fig. 3. Cross section of the evaporator tube in the boiling zone.

By differentiation with respect to P we obtain:

$$\frac{dT}{dP} = n.c.P^{n-1} \tag{42}$$

Introduction of Equation 42 in Equation 41 leads to:

$$U_z = \frac{1}{\pi.D.L(P_s^n - P^n)}\left[\frac{\lambda}{c}\,\frac{dW_2}{dZ*} + (W_1.Cp_1 + W_2.Cp_2)n.P^{n-1}\frac{dP}{dZ*}\right] \tag{43}$$

Equation 43 will be solved numerically together with Equation 37. This will give values of the local heat transfer coefficient for the boiling zone. These values of U_z, after being correlated, will be used in the testing of the model to evaluate $dW_2/dZ*$.

V. RESULTS

A. *Liquid zone.*

1. Experimentation under atmospheric pressure.

Seven different flow rates of water were used, the system was kept at atmospheric pressure and the steam pressure set at 1.357 10^5 Pa absolute. When a steady state was reached, the temperature was recorded for a period of at least 15 min. An average value of the temperature read by each of the 7 thermocouples over this period was taken. The temperature fluctuation, which was nil for thermocouples 1 and 2, increased with the distance to reach a value of 1°C at thermocouple 7 (exit temperature)

The temperature profile along the tube as a function of the distance z is shown for different flow rates in Figure 4. From Figure 4 it appears that the lower part of the exchanger tube does not seem to be effective; this was probably due to the fact that the flow was laminar prior to the heat transfer zone and the thermocouples placed at the center of the tube did not record any temperature change. After a short length of heating, the tube being vertical, convection occurred and the velocity profile was no longer parabolic.

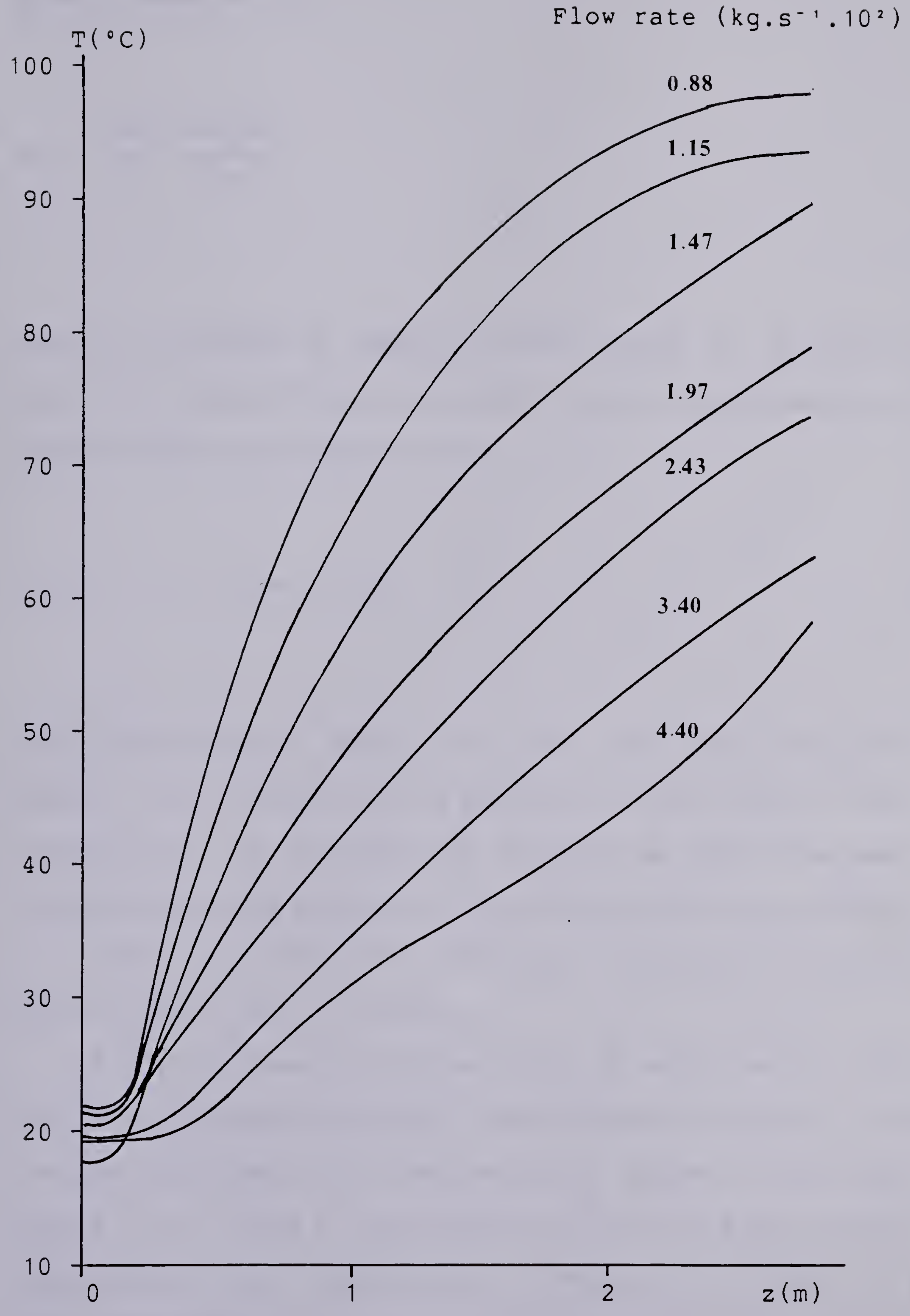

Fig. 4. Temperature profile in the liquid zone.

Recall Equation 12:

$$Nu_z = \frac{Pe_i}{4} \frac{d\ln(T*)}{dZ*}$$

Looking at Figure 5, showing ln(T*) versus Z*, we can see that for a given flow rate ln(T*) can be approximated by a second degree polynomial in Z*:

$$\ln(T*) = A + B.Z* + C.Z*^2 \qquad (44)$$

The coefficients A, B and C for each flow rate are given in Table 1. Z_0* is the root of Equation 44 when T*=1 in the interval [0, 1]. It gives the distance at which the heat transfer apparently starts and reflects entrance effects.

The inlet conditions are known, therefore the initial Peclet Number (Pe_i) is known.

Figure 6 shows the values of A, B and C versus $1/Pe_i$. The lines represent the best least squares fit of A, B and C function of $1/Pe_i$ for a regression of degree 1 for A and degree 2 for B and C. The squares of multiple correlation coefficients are, respectively, 0.992 for A, 0.9995 for B and 0.9985 for C.

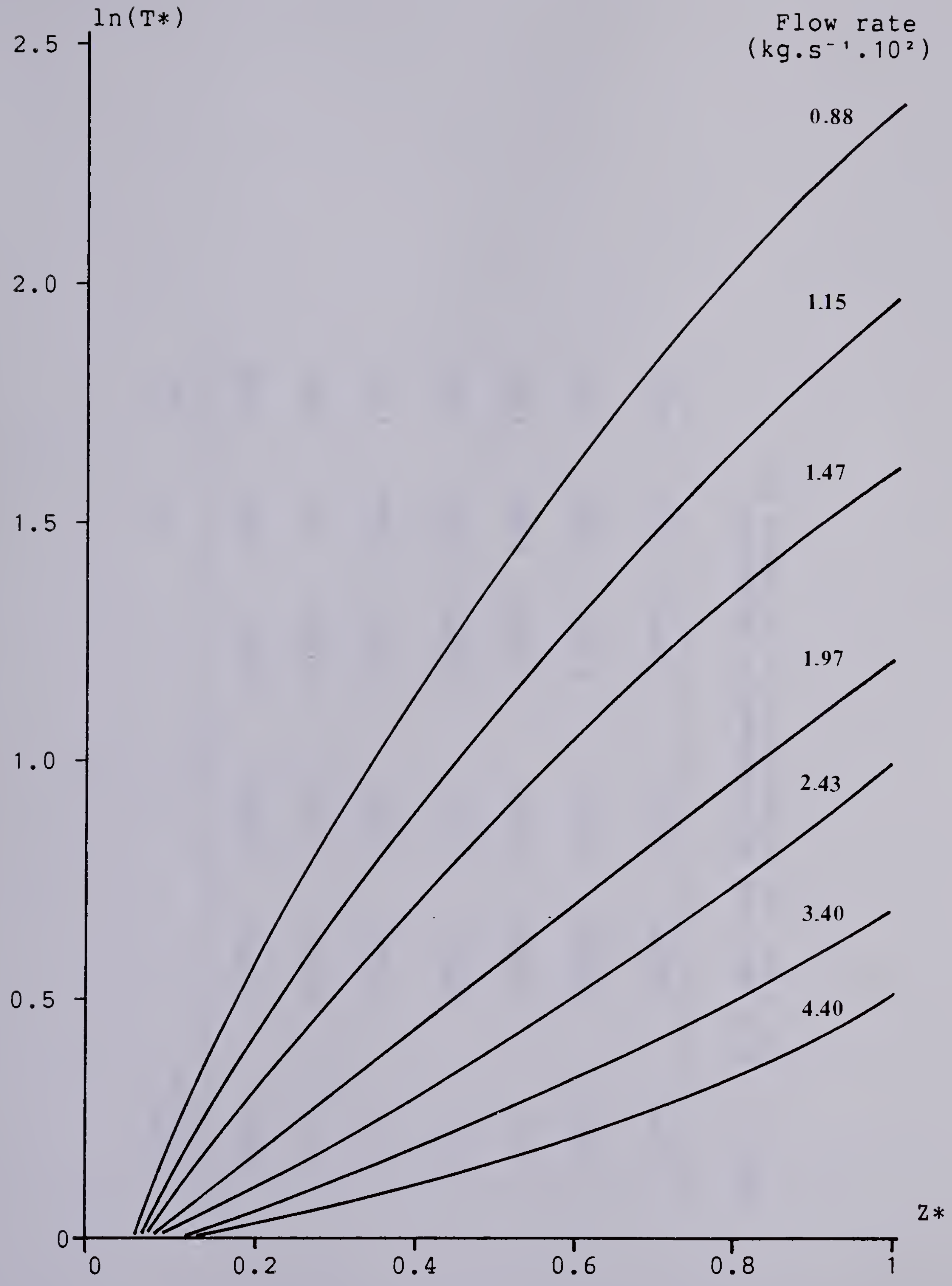

Fig. 5. Liquid zone: ln of the dimensionless temperature T* versus the dimensionless position Z*

W $kg.s^{-1}.10^{2}$	A	B	C	Z_0*	z_0 cm
0.88	−0.170	3.888	−1.425	0.044	11.85
1.15	−0.133	2.746	−0.6845	0.049	13.08
1.47	−0.0958	1.963	−0.2803	0.049	13.12
1.97	−0.0617	1.312	−0.0546	0.047	12.67
2.43	−0.0443	0.8881	0.1302	0.050	13.23
3.40	−0.0353	0.5216	0.1818	0.066	17.67
4.40	−0.0249	0.3170	0.2059	0.075	20.02

Table 1. A, B and C are the coefficients of Equation 44.
Z_0* is the root of Equation 44 in the interval [0, 1]

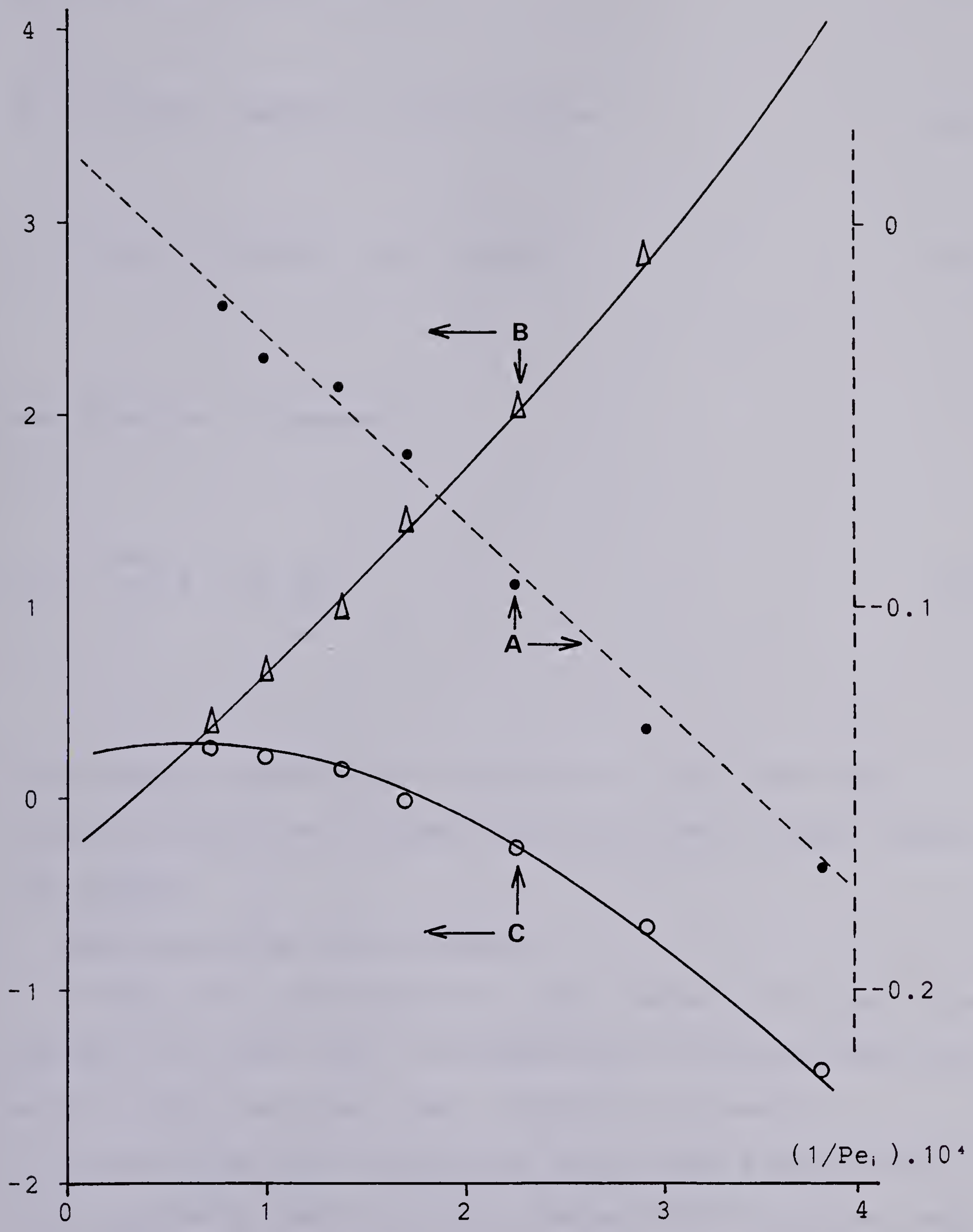

Fig. 6. Coefficients A, B and C from Equation 44 vs 1/Pe$_i$. The curves represent the best least squares fit.

$$A = 0.01698 - 494.9/Pe_i \qquad (45)$$

$$B = -0.458 + 9445/Pe_i + 5.22\ 10^6/Pe_i^2 \qquad (46)$$

$$C = 0.238 + 755/Pe_i - 135\ 10^7/Pe_i^2 \qquad (47)$$

Now Equation 12 becomes:

$$Nu_z = \frac{Pe_i}{4}(B + 2C.Z*) \qquad (48)$$

This equation permits the evaluation of the local heat transfer coefficient in the liquid zone when no gas bubbles are present.

2. Experimentation under vacuum.

When using the evaporator under vacuum with water from the tap, we found that the temperature increases faster and earlier than predicted under atmospheric pressure.

Looking at the liquid zone, we can see a multitude of tiny bubbles of gas which are released from the water under vacuum. If we degassed the water before evaporation, the temperature profile under vacuum remained the same as for atmospheric pressure, as shown in Figure 7. The heat transfer in the liquid zone is increased by the presence of

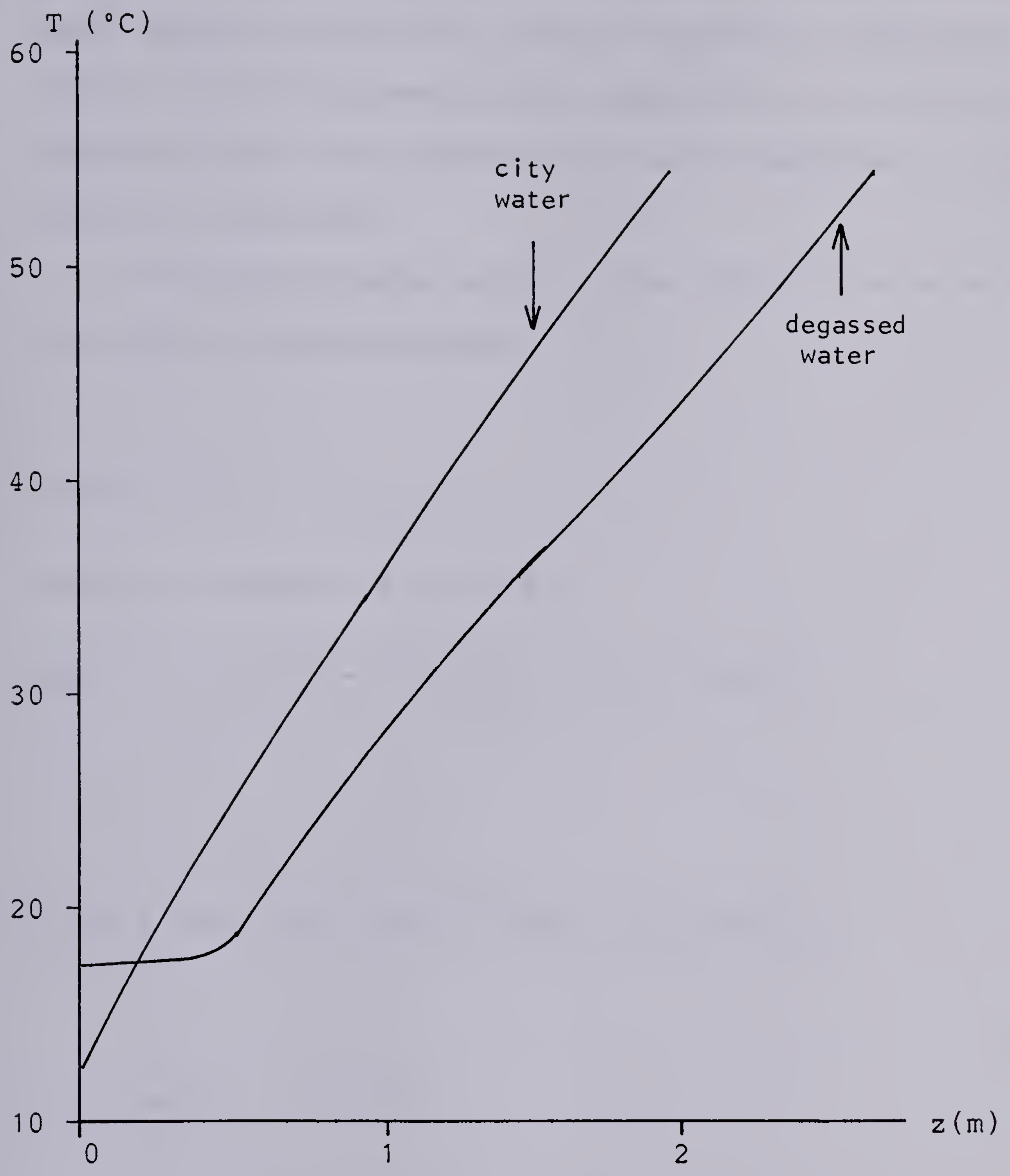

Fig. 7. Comparison of the temperature profiles in the liquid zone between tap water and degassed water. The flow rates are identical.

gas in solution at atmospheric pressure which is released under vacuum to form tiny bubbles creating turbulence in the liquid. Unlike the atmospheric pressure case or when using degassed water, the temperature rises immediately at the bottom of the tube.

A new set of equations for the liquid zone using water from the tap was developed:

$$\ln(T*) = Z* \, (B_1 + C_1 . Z*) \tag{49}$$

$$\text{with } B_1 = 0.3851 - 6739.3/Pe_i \tag{50}$$

$$\text{and } C_1 = -0.081 - 1719/Pe_i + 3.12\ 10^7/Pe_i{}^2 \tag{51}$$

In this case the Nusselt Number is given by:

$$Nu_z = \frac{Pe_i}{4}(B_1 + 2C_1 . Z*) \tag{52}$$

This equation permits the evaluation of the local heat transfer coefficient in the liquid zone when gas bubbles are released under vacuum.

Equation 44 or 49 will be used in the testing of the model to determine when the boiling temperature is reached.

B. *Boiling zone.*

In the Theory section we developed the equations controlling the pressure drop, the void fraction and the heat transfer in the boiling zone. Now we have to solve these equations to see if they lead to values consistent with the experiment.

Experimentation in the boiling zone was conducted with water entering the tube at a temperature corresponding to the boiling point in the system (dependent on the vacuum).

Both heat transfer and pressure drop equations contain the mass flow rate of liquid phase and vapor phase which are a function of the position in the tube. The only positions where we know these values by experiment are at the inlet and at the oulet of the evaporator tube.

As suggested by Wallis (1969), we can assume that the quality increases linearly with the distance, therefore the mass flow rate of the vapor increases linearly with the distance:

$$W_2 = Z^* . W_2\text{exit} \tag{53}$$

Differentation with respect to Z* gives:

$$\frac{dW_2}{dZ^*} = W_2\text{exit} \tag{54}$$

Now Equation 37 can be solved numerically using a 4th order Runge Kutta method to obtain local values of the pressure along the tube. Then the temperature in the vapor phase can be calculated from Equation 31.

As the distance Z* is incremented at each step of the numerical integration, a local heat transfet coefficient U_z is evaluated from Equation 43.

The detailed computer program is given in Appendix B.

Figure 8 shows the approximate temperature profile obtained by numerical solution compared to the experimental temperatures from Table 2. The values of the local heat transfer coefficient U_z obtained from all data (variation of feed rate, variation of steam pressure, variation of vacuum: Tables 2, 3 and 4) appeared to be the same for a given position Z*. Table 5 show the mean and the standard deviation of the estimated values of U_z while Figure 9 represents the best least squares fit of the average heat transfer coefficient versus Z* for a regression of degree 2. (square of multiple correlation coefficient = 0.9999).

$$U_z = 615.5 - 112\ Z^* + 41.55\ Z^{*2} \tag{55}$$

U_z can be also related to α in the following way:

$$U_z = 615.5\ \mathrm{W.m^{-2}.K^{-1}} \quad \text{for } \alpha < 0.64$$

$$U_z = 805.44 - 295.4\ \alpha \quad \text{for } 0.64 < \alpha < 1 \tag{56}$$

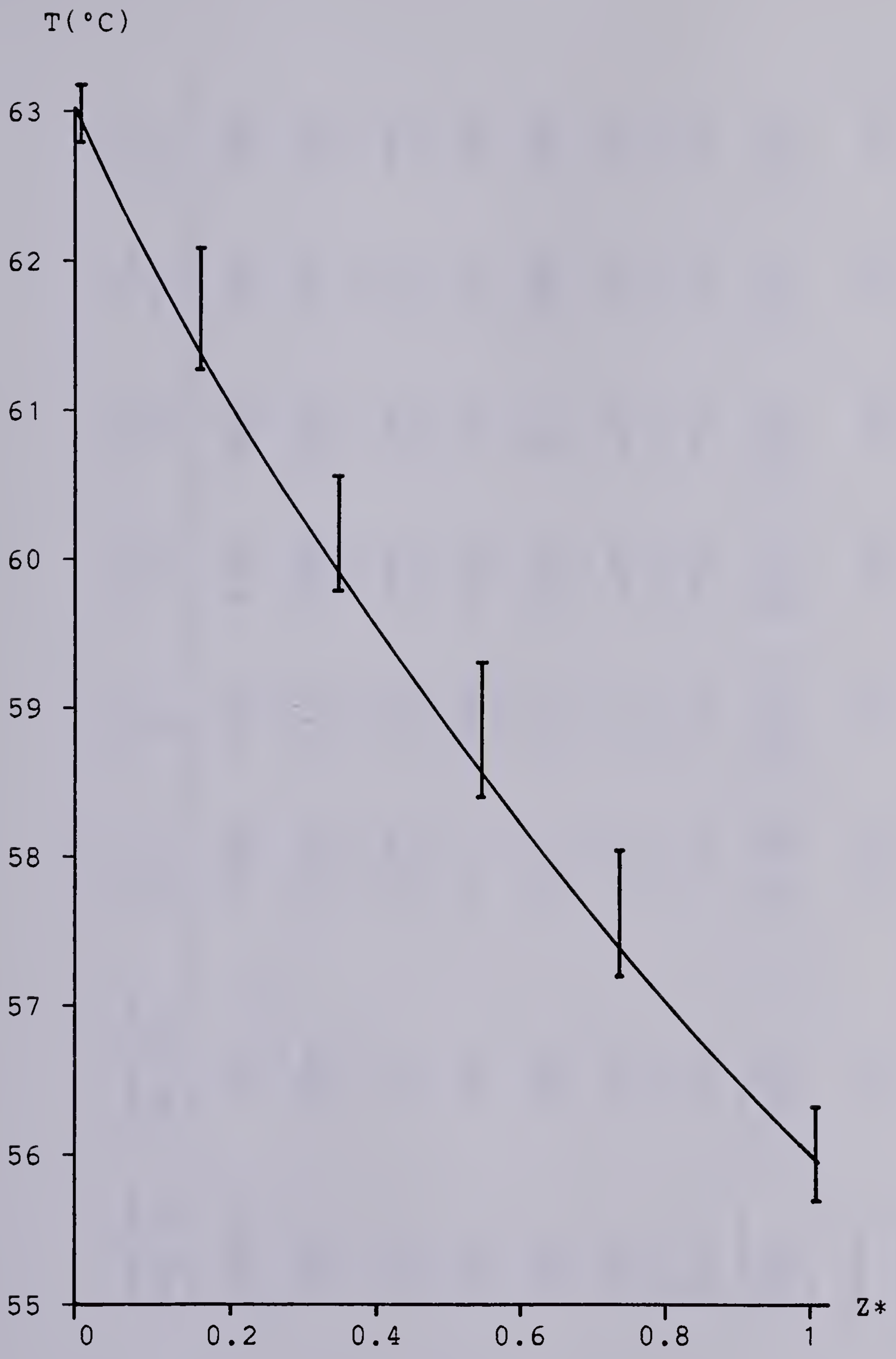

Fig.8. Temperature profile in the boiling zone: The solid curve represents the numerical solution. The vertical lines represent the experimental values as per Table 2.

Feed rate $kg.s^{-1}.10^3$	Vapor rate $kg.s^{-1}.10^3$	T.C.2 ^0C	T.C.3 ^0C	T.C.4 ^0C	T.C.5 ^0C	T.C.6 ^0C	T.C.7 ^0C
6.925	3.13	62.9	61.5	60.0	58.8	57.5	56.2
9.93	3.09	63.0	61.3	59.8	58.3	57.3	55.8
13.05	3.18	62.9	61.5	59.8	58.6	57.5	55.8
13.85	2.93	63.1	61.5	60.2	58.8	57.7	55.6
17.02	2.92	63.1	61.7	60.2	59.1	58.0	56.0
19.87	2.93	62.9	62.0	60.5	59.3	58.0	56.0
26.10	3.03	63.0	62.0	60.5	59.2	58.0	55.9
Mean	3.03	62.99	61.64	60.14	59.87	57.74	55.90
Standard deviation	0.107	0.078	0.27	0.25	0.35	0.25	0.19

Table 2. Temperature profiles in the boiling zone for seven different feed rates. The steam pressure and the vacuum remain the same.

Steam pres. Pa.10^{-5}	Vapor rate kg.$s^{-1}.10^{3}$	T.C.2 ^{0}C	T.C.3 ^{0}C	T.C.4 ^{0}C	T.C.5 ^{0}C	T.C.6 ^{0}C	T.C.7 ^{0}C
1.116	2.69	62.2	60.5	58.8	57.7	56.3	54.8
1.288	3.14	62.4	60.9	59.4	58.0	56.8	55.3
1.426	3.24	62.4	60.8	59.2	58.3	57.0	55.3
1.564	3.48	62.3	60.5	59.0	58.5	57.0	55.6
1.702	3.49	62.2	60.7	59.2	58.5	57.3	55.7

Table 3. Temperature profiles in the boiling zone for different steam pressures. The vacuum and the feed rate remain the same.

Vacuum Pa.10^{4}	Vapor rate kg.s^{-1}.10^{3}	T.C.2 ^{0}C	T.C.3 ^{0}C	T.C.4 ^{0}C	T.C.5 ^{0}C	T.C.6 ^{0}C	T.C.7 ^{0}C
2.215	3.14	62.3	60.8	59.5	58.5	56.9	55.4
2.775	2.74	68.0	66.8	65.5	64.5	63.5	62.0
3.415	2.30	73.5	72.0	71.5	70.3	69.3	68.3
3.936	2.08	76.9	76.0	75.0	74.3	73.5	72.3
4.269	1.93	78.6	78.0	77.1	76.2	75.3	74.3

Table 4. Temperature profiles in the boiling zone for different vacuums. The steam pressure and the feed rate remain the same.

Z^*	$\overline{U_z}$	Standard deviation	$\overline{\alpha}$
0.1	604.69	24.8	0.698
0.2	594.71	23.6	0.719
0.3	585.56	23.9	0.741
0.4	577.24	23.7	0.763
0.5	569.80	23.6	0.785
0.6	563.20	23.7	0.809
0.7	557.40	23.9	0.832
0.8	552.45	24.3	0.854
0.9	548.30	24.8	0.877
1.0	544.90	25.5	0.898

Table 5. Mean and standard deviation of the heat transfer coefficient in the boiling zone from experiments as per Tables 2, 3 and 4.

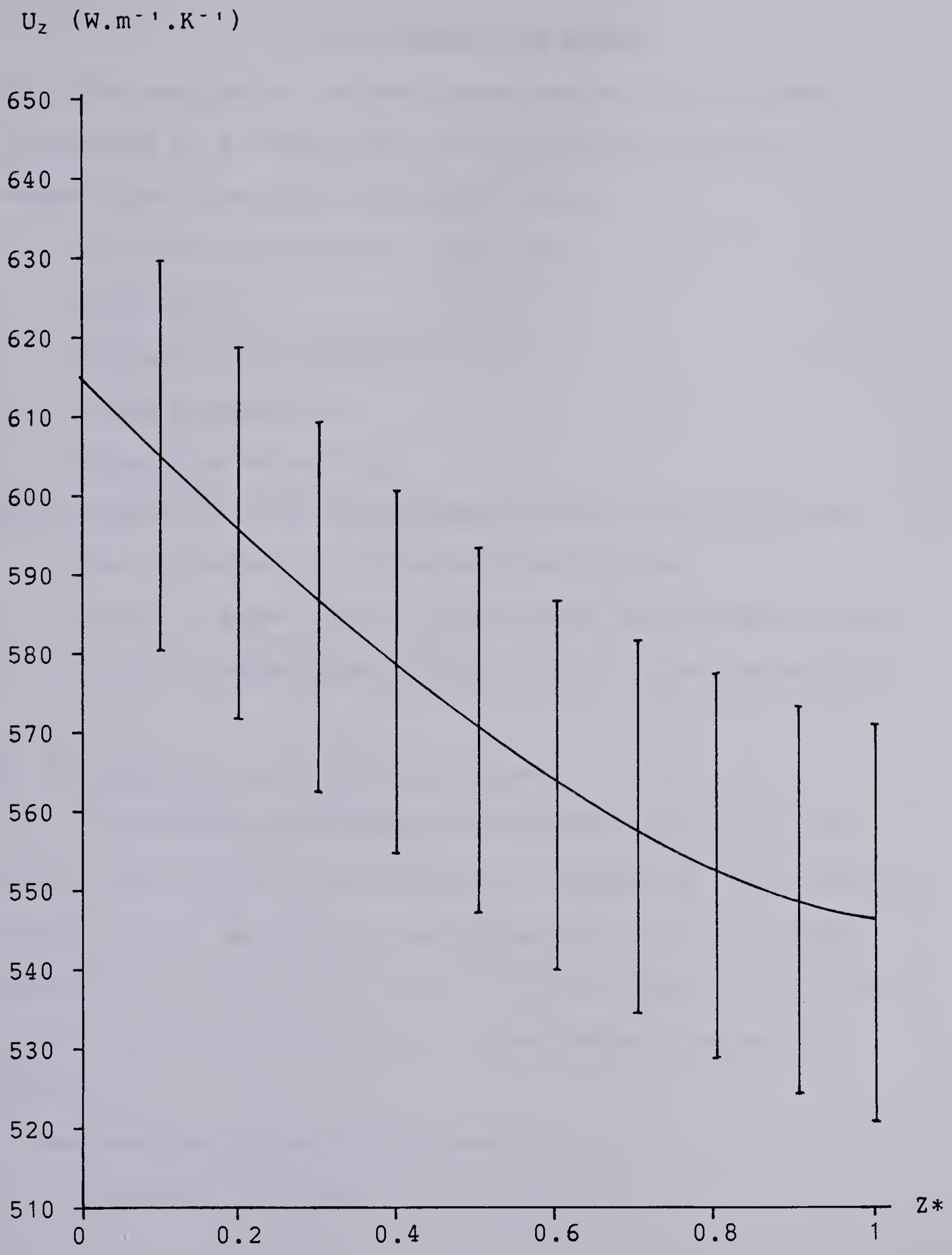

Fig. 9. Best least squares fit of the heat transfer coefficient in the boiling zone.

VI. TESTING THE MODEL

When the evaporator is used under vacuum and the feed introduced at a temperature lower than the boiling temperature, the known parameters are:

- -initial conditions (T , Cp , k_i)
- -feed rate W.
- -vacuum in the system P_v.
- -steam pressure P_s.
- -Equations 44 and 49.

The parameters to be determined are the following ones:

- -Zb* = distance at which boiling starts.
- -W_2exit = vapor rate at the outlet of the evaporator.
- -Texit = temperature at the outlet of the evaporator.

A. *Distance at which boiling starts.*

To determine the temperature profile in the liquid zone, depending on the presence or absence of gas released under vacuum, we have to solve Equation 12 using either Equation 44 (no gas) or Equation 49 (with gas) to evaluate ln(T*) as a function of the initial Peclet Number and position.

1. No bubbles in the liquid zone.

Equation 12 gives:

$$\int_{1}^{T*} d\ln(T*) = \frac{4}{Pe_i}\int_{Z_0*}^{Z*} Nu_z . dZ* \qquad (57)$$

Introduction of Equation 44 gives:

$$\ln(T^*) = \frac{4}{Pe_i}\int_{Z_0^*}^{Z^*} \frac{Pe_i}{4}\,(B + 2C.Z^*)dZ^*$$

Integration with respect to Z* gives:

$$\ln(T^*) = [B.Z^* + C.Z^{*2}]_{Z_0^*}^{Z^*} \tag{58}$$

$$\ln(T^*) = -B.Z_0^* - C.Z_0^{*2} + B.Z^* + C.Z^{*2} \tag{59}$$

The computer program of Appendix C shows the case when no gas is released.

The coefficient A is evaluated from an average value of Z_0^* for the five lower flow rates as given in Table 1:

$A = - Z_0^*(B + C.Z_0^*)$

The values for the two higher flow rates were not used because such high flow rates are not encountered when using the evaporator under vacuum; the temperature at the exit being lower than the boiling point, therefore no evaporation occurs in the tube.

-From the vacuum in the system we know the temperature at which boiling starts (the vapor follows the saturation

curve).

-The boiling point rise due to the concentration of the feed has to be added when not using pure water.

-Solution of Equation 59 for that temperature gives us the distance Zb* at which the boiling zone begins.

2. Bubbles released in the liquid zone.

Introduction of Equation 49 in Equation 57 gives:

$$\ln(T^*) = \int_0^{Z^*} (B_1 + 2C_1 . Z^*) dZ^* \qquad (60)$$

Integration with respect to Z* gives:

$$\ln(T^*) = B_1 . Z^* + C_1 . Z^{*2} \qquad (61)$$

Solution of Equation 61 for the boiling temperature as defined earlier gives us the distance Zb* at which boiling starts.

B. *Temperature and vapor rate in the boiling zone.*

In the Results section, we used the experimental value of W_2exit to determine dW_2/dZ^*. Now dW_2/dZ^* is unknown and we have to use Equation 43 to determine the change of vapor flow rate with the position:

$$\frac{dW_2}{dZ*} = \frac{\pi.D.c.L.U_z}{\lambda}(P_s^n - P^n) - \frac{(W_1.Cp_1 + W_2.Cp_2)n.c.P^{n-1}}{\lambda}\frac{dP}{dZ*} \quad (62)$$

with U_z given by Equation 55.

-starting at Z*=Zb* we solve numerically Equations 37 and 62 using a double Runge Kutta 4th order method.

-When Z*=1 is reached, we know the pressure at the exit, therefore the temperature, and we know the vapor rate W_2exit.

The computer program to evaluate these parameters is given in Appendix C.

Table 6 shows the comparison of experimental results with the results obtained from the model using Equation 49 in the liquid zone and city water as medium.

We can see that the agreement is very good, the maximum difference for the distance at which boiling starts being 3.5% while the maximum difference on the vapor rate at the exit of the evaporator is 4.43%.

Table 7 shows results obtained for degassed water using Equation 44 in the liquid zone.

Even when using degassed water, the boiling starts a little bit earlier than predicted numerically, probably because some gas is still present in the feed (the feed tank being held at atmospheric pressure, some gas went back into solution during the process).

Feed rate W $kg.s^{-1}.10^2$	Boiling starts at Zb* =			W_2 exit $kg.s^{-1}.10^2$			T exit (^0C)	
	est.	obs.	%dif.	est.	obs.	%dif.	est.	obs.
0.692	0.156	0.154	1.3	0.269	0.263	2.3	55.9	55.7
0.993	0.220	0.228	-3.5	0.251	0.247	1.6	56.2	55.6
1.305	0.286	0.277	3.3	0.233	0.239	-2.6	56.2	55.8
1.385	0.302	0.307	-1.6	0.228	0.221	3.0	56.3	56.0
1.987	0.421	0.431	-2.3	0.191	0.183	4.4	57.2	56.0

Table 6. Comparison between experimental values and values predicted by the model for tap water.

Product	Feed rate kg.s^{-1}.10^{2}	Zb* =			W$_2$ exit (kg.s^{-1}.10^{2})			T exit (°C)	
		est.	obs.	%dif.	est.	obs.	%dif.	est.	obs.
Deg. water	0.692	0.195	0.185	5.4	0.254	0.258	−1.6	53.7	53.9
Deg. water	0.983	0.280	0.268	4.5	0.228	0.233	−2.1	54.2	53.5
Deg. water	1.383	0.399	0.367	8.7	0.192	0.196	−2.1	54.9	53.4
Deg. water	1.667	0.494	0.457	8.1	0.162	0.177	−8.5	55.6	53.5
Sucr. (17%)	1.080	0.265	0.245	8.2	0.231	0.241	−4.2	54.8	54.2
Sucr. (23%)	0.812	0.196	0.185	5.9	0.252	0.260	−3.1	54.2	54.8
Sucr. (33%)	0.700	0.171	0.167	2.4	0.261	0.243	7.4	53.7	55.7
Sucr. (40%)	0.800	0.197	0.190	3.7	0.252	0.253	−0.4	53.9	55.7
Tom. juice	1.300	0.277	0.277	0.0	0.218	0.225	−3.1	57.5	56.5

Table 7. Comparison between experimental values and values predicted by the model for degassed water and different liquid solutions.

C. *Testing with liquid food.*

The model was tested with sucrose solutions of different concentrations and tomato juice. We chose tomato juice because it is well known in the food industry as being a product difficult to evaporate due to the high proportion of pulp it contains. The results are shown in Table 7.

The sucrose solutions were not degassed and the difference in the boiling position between experiment and calculation decreased when the concentration of the feed increased. This is due to the viscosity effect; the more viscous the product is, the more difficult it is for the gas to be released.

For tomato juice we could not use the rotameter because of the pulp present in the feed and the color. The feed rate was determined by recording the decrease in weight of the feed tank during the process.

Even with the problems created by the release of gas bubbles in the liquid zone under vacuum, we can see from Table 7 that the differences between the experimental values and the computed values for the distance at which boiling starts and for the vapor rate at the exit of the evaporator is always below 10%. This is very good considering that the error on the feed rate reading can be 3% and the error on the concentrate rate is between 2% and 5% depending on the rate at which condensate enters the receiver. The error on the vapor rate, observed experimentally at the exit, is then between 5% and 8%.

VII. DISCUSSION OF RESULTS

A. *Liquid zone.*

In the development of the equations to determine the heat transfer in the liquid zone, the Peclet Number came out naturally during the dimensionalization of the equations.

All the initial conditions are known: temperature of the feed, feed rate, heat capacity and thermal conductivity of the feed at the inlet temperature; but some of these quantities vary along the tube and are therefore unknown for a position $Z* \neq 0$. This is why it is advantageous to develop the equations using the initial Peclet Number (Pe_i), for it is the only Peclet Number we can calculate and the one which will reflect the initial conditions.

In the liquid zone, we obtained two equations correlating the Nusselt Number to the initial Peclet Number and the position Z*. These two equations are of a similar form but differ in their coefficients. This is due to the fact that we used the thermal conductivity of liquid water in both cases, while, when gas bubbles are present, the real value is somewhere between the thermal conductivity of the liquid and the thermal conductivity of the gas.

In Chapter 13 of Bird *et al.* (1960), the solution to the Graetz equation, as proposed by Lévêque, applies to laminar flow in pipes. It is as follows:

$$Nu_{ln} = 1.62(Re.Pr.D/L)^{0.33}$$

with $Nu_{ln} = h_{ln}.D/k$

In our case the Nusselt Number is also a function of the Peclet Number (Re.Pr). The flow in the liquid zone being laminar, this supports the validity of our model because the equation we developed is similar to the Lévêque equation.

In the liquid zone when the system is under atmospheric pressure or when using degassed water, we found that the temperature at the center does not increase immediately. All the flow rates investigated correspond to the laminar flow zone (Re < 2100). As is well known, the velocity profile is parabolic for laminar flow in tubes. The temperature profile for radial heat flow from the wall of a tube is laminar as well; this explains why the thermocouple which is situated at 15 cm from the beginning of the steam jacket at the center of the tube records almost the same temperature as the thermocouple located before the heating zone. However, after a short distance of heating, natural convection occurs and the velocity and temperature profiles are modified. In Figure 10 the solid curve represents the parabolic velocity profile encountered in laminar flow, while the short dotted curve represents the theoretical velocity profile which would be encountered in the heated tube filled with water (with a zero flow rate) subject to natural convection. The long dotted curve represents the resultant velocity profile

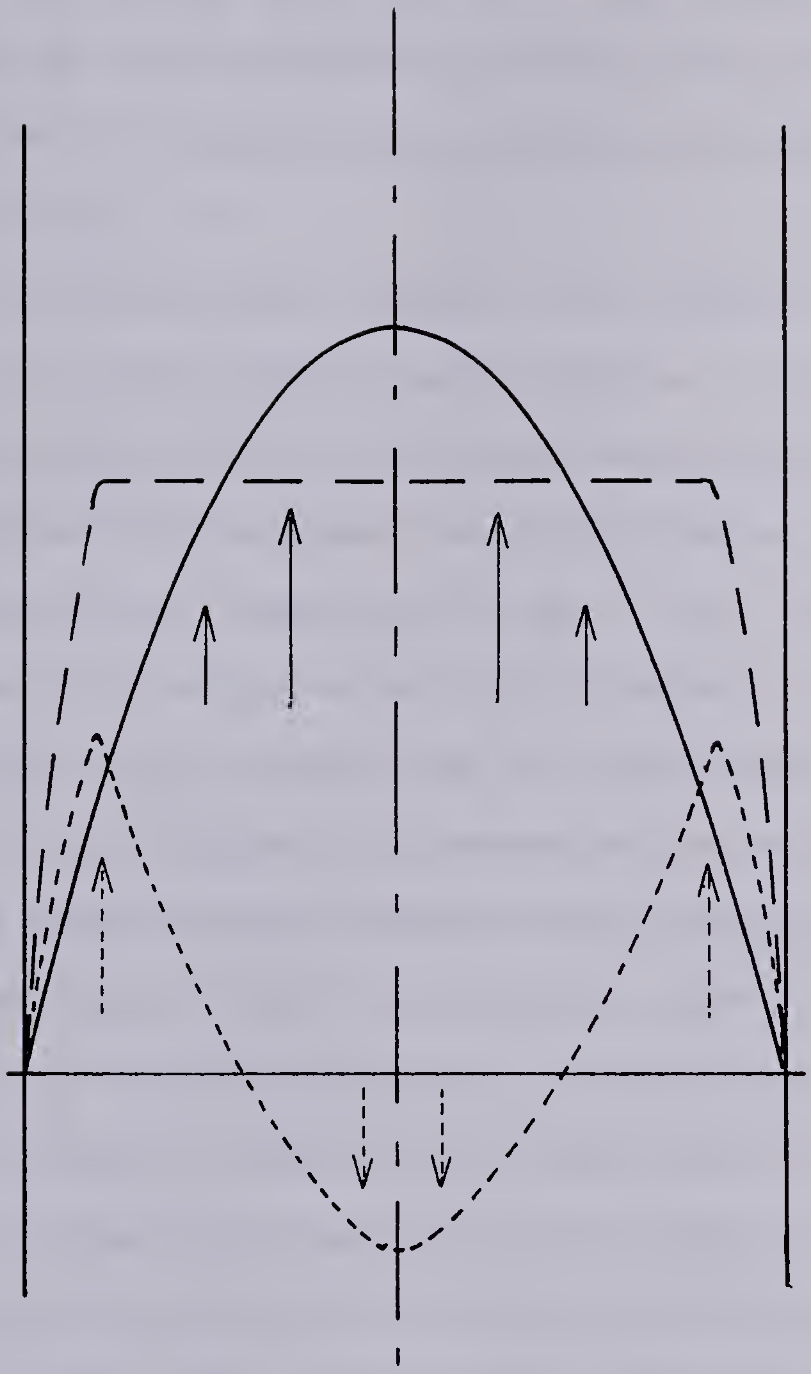

Fig. 10. Temperature profiles in the liquid zone.
Solid curve = Laminar flow profile.
Short dotted curve = natural convection profile.
Long dotted curve = resultant profile.

which is supposed to occur in the tube after a certain distance of heating. It can be seen that this profile, which is the sum of the two previous ones, is no longer parabolic and is close to the velocity profile encountered in turbulent flow.

When working under vacuum, the release of the dissolved gases prior to the heating zone creates a turbulent flow velocity profile before the liquid enters the evaporator tube, and then the temperature at the center rises immediately as confirmed by Figure 7. This phenomenon is not as critical for solutions of high viscosity, like sugar solutions and tomato juice, as for water because the rising velocity of the bubbles is lowered by the viscous drag and for highly concentrated sucrose solutions and tomato juice the bubbles travel almost at the same speed as the liquid, reducing their agitation effect on the velocity profile.

In the Results section, the model was validated using water. The dimensionalization of the equations was done to take into account the influence of the change in physical properties which will appear when using other liquid products (viscosity, heat capacity, density and thermal conductivity). This is why the model gave good agreement with the experimental values when tested with sucrose solutions and tomato juice.

B. *Boiling zone.*

In the boiling zone a first attempt at modeling was made using the equations proposed by Wallis (1969) which are concerned with separated flow with phase change. The model did not work regardless of the repartition of the force for momentum increase due to phase change between Stream 1 and Stream 2. The obtained pressure drop was always too high and the corresponding temperature at the exit of the evaporator too low. Even in some cases the predicted exit temperature was negative (below freezing).

In the equations proposed by Wallis, the drag force exerted by the tube wall on the vapor and on the liquid and the drag force between the two components (liquid and vapor) have to be evaluated using the Lockhart and Martinelli (1949) correlation which was established for isothermal two-phase, two-component flow without phase change. In our case these two hypotheses cannot be made: the flow is not isothermal and the phase change is very important.

The equations proposed by Malnes (1975) were investigated together with the assumption made by Levy (1960) that, when the rate of evaporation is rapid enough, friction and body terms can be neglected as compared to inertia and phase change.

We made the same assumption as Malnes that the slip ratio stays constant.

The slip ratio, S, is given by: $S=V_2/V_1$

The introduction of V_1 and V_2 as per Equations 20 and 21 gives:

$$S = \frac{\rho_1}{\rho_2} \frac{G_2}{G_1} \frac{(1 - \alpha)}{\alpha}$$

The mass fluxes are related to the mass flow rates as follows:

$$G_1 = W_1/(\pi.D^2/4) \quad \text{and} \quad G_2 = W_2/(\pi.D^2/4)$$

We have now:

$$S = \frac{\rho_1}{\rho_2} \frac{W_2}{W_1} \frac{(1 - \alpha)}{\alpha}$$

We can see that an increase in W_2 is compensated by an increase in α, while the decrease in the value of W_1 is compensated by a decrease in $(1 - \alpha)$. Then the expression $W_2/W_1.(1-\alpha)/\alpha$ remains constant.

The slip ratio is then proportional to ρ_1/ρ_2 which can be assumed constant for a given experiment.

For this model the void fraction had to be determined from another equation. The Darmouth correlation modified by Turner (1966) was appropriate because it is given for vertical upward cocurrent annular flow. It is developed assuming that the regime in the annular flow presents viscous and surface-tension forces which are small, and the fluid dynamics are governed by a balance between hydrostatic forces and inertia forces in the gas and the liquid. This is compatible with the assumption made by Levy (1960) that inertia and phase change terms are usually much larger than friction and body terms when rapid evaporation occurs in the tube.

This choice of calculation for α was further supported by the fact that all our experimental values for the dimensionless volumetric fluxes j_1* and j_2* were within the graph given by Wallis (1969) representing the range for which the equation proposed by Turner (1966) is valid.

C. *About the computer programs.*

In the numerical evaluation of the pressure in the boiling zone (see Appendix B) the step size used in the Runge-Kutta method was set at 1/20. This choice is not an arbitrary one. A series of tests were made on the same set of data for different step sizes of 1/5, 1/10, 1/20 and 1/50. The numerical values of pressure, heat transfer coefficient and void fraction at the exit of the evaporator ($Z*=1$) were compared. The difference between values obtained

for a step size of 1/5 and values obtained for a step size of 1/10 was about 10%; the difference between a step size of 1/10 and a step size of 1/20 was 2%; while the difference between a step size of 1/20 and a step size of 1/50 was less than 0.3%. A difference of 0.3% being a lot smaller than the precision we have on experimental data, a step size of 1/20 was chosen. A step size of 1/50 could have been used, but it would have required more computing time and greater expense for a gain in precision which is not significant. As stated earlier (Testing the model section), the error on the vapor rate observed experimentaly at the exit of the evaporator is between 5% and 8%.

In Appendix C a step size of (1-Zb*)/20 is used. This is smaller than 1/20 and we are sure that the precision of the numerical solution is at least as good as the one obtained in Appendix B.

VIII. APPLICATION TO AN INDUSTRIAL SIZE EVAPORATOR

Data for an industrial size evaporator were provided by Dr. Merson of the Department of Food Science and Technology, University of California, Davis, California. They are summarized in Figure 11.

A. *Description of the evaporator.*

A schematic diagram of the evaporator to be studied is given in Figure 11.

This evaporator is used to concentrate pineapple juice from 13.5°Brix to 62°Brix at a rate of approximately 5,000 kg/hr.

As can be seen on the diagram, the evaporator is composed of 3 consecutive sections, each section having more tubes than the preceeding one to permit expansion of the vapor and ensure a climbing film pattern during the entire process.

The only known parameters are the inlet conditions, the outlet conditions and the characteristics of the evaporator (tube diameter, length, thickness and number).

The feed is preheated before entering the evaporator (115°C).

The pressure at the outlet is known (495mm Hg). The pressure at the inlet of the evaporator is unknown, and an appropriate value can be estimated by analogy with our single tube glass evaporator. The average pressure drop in our glass evaporator is 47.6mm Hg for the 2.67m length. The

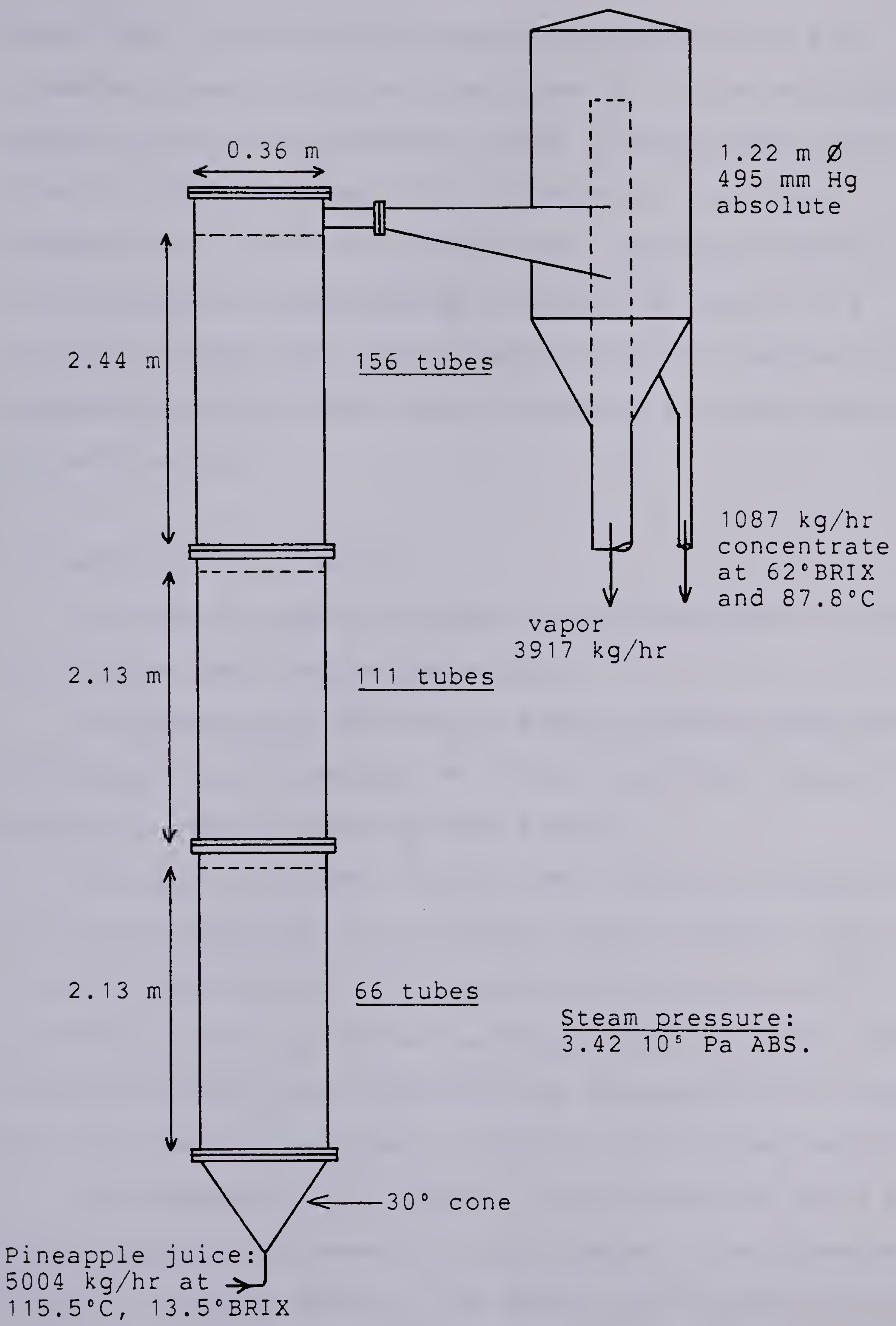
0.36 m
1.22 m Ø
495 mm Hg
absolute
2.44 m
156 tubes
1087 kg/hr
concentrate
at 62°BRIX
and 87.8°C
vapor
3917 kg/hr
2.13 m
111 tubes
2.13 m
66 tubes
Steam pressure:
3.42 10⁵ Pa ABS.
30° cone
Pineapple juice:
5004 kg/hr at
115.5°C, 13.5°BRIX

Fig. 11. Schematic diagram of the industrial evaporator.

added tube length of the industrial evaporator is 6.7m; the expected pressure drop will be close to 119.5mm Hg, which added to the outlet pressure, gives an approximate inlet pressure of 614.5mm Hg. This corresponds to an inlet temperature of 94°C. Because of that, flashing occurs in the conical section preceding the first set of tubes, so a mixture of vapor and liquid reaches the first section of the evaporator and two phase flow is present all along the tubes in each section.

B. *Method of calculation.*

In order to apply our model to that evaporator we have to consider each section separately.

We assume that the flow is equally distributed among the tubes in each section. We divide the total flow by the number of tubes present in that section.

We apply the model for one tube (after modification for the characteristics of that tube: length, diameter and heat transfer coefficient). This permits one to evaluate the pressure at the top of that section, while the vapor and concentrate rates are determined by multiplying the results for one tube by the number of tubes in that given section.

The composition at the exit of that section being known (void fraction and density of both phases), the pressure drop in the space between tube sheets from one section to the next one can be evaluated. Assuming homogenous two-phase flow, the pressure drop between sections is given by:

$$\Delta P = H[\alpha.\rho_2 + (1 - \alpha)\rho_1].g \tag{63}$$

with $H = 0.153m$

1. Evaluation of the amount of flashing.

The amount of flashing prior to the first section of the evaporator is not known, and the composition of the feed (ratio of vapor to liquid) and the temperature at the beginning of the evaporation process are unknown.

The only parameter available is the pressure at the exit of the evaporator, therefore the temperature is known (the vapor phase is assumed to follow the saturation curve).

An iterative evaluation converging on the outlet temperature has to be used. It works as follow:

The initial conditions prior to the inlet of evaporator are known: Temperature, feed rate, degree Brix.

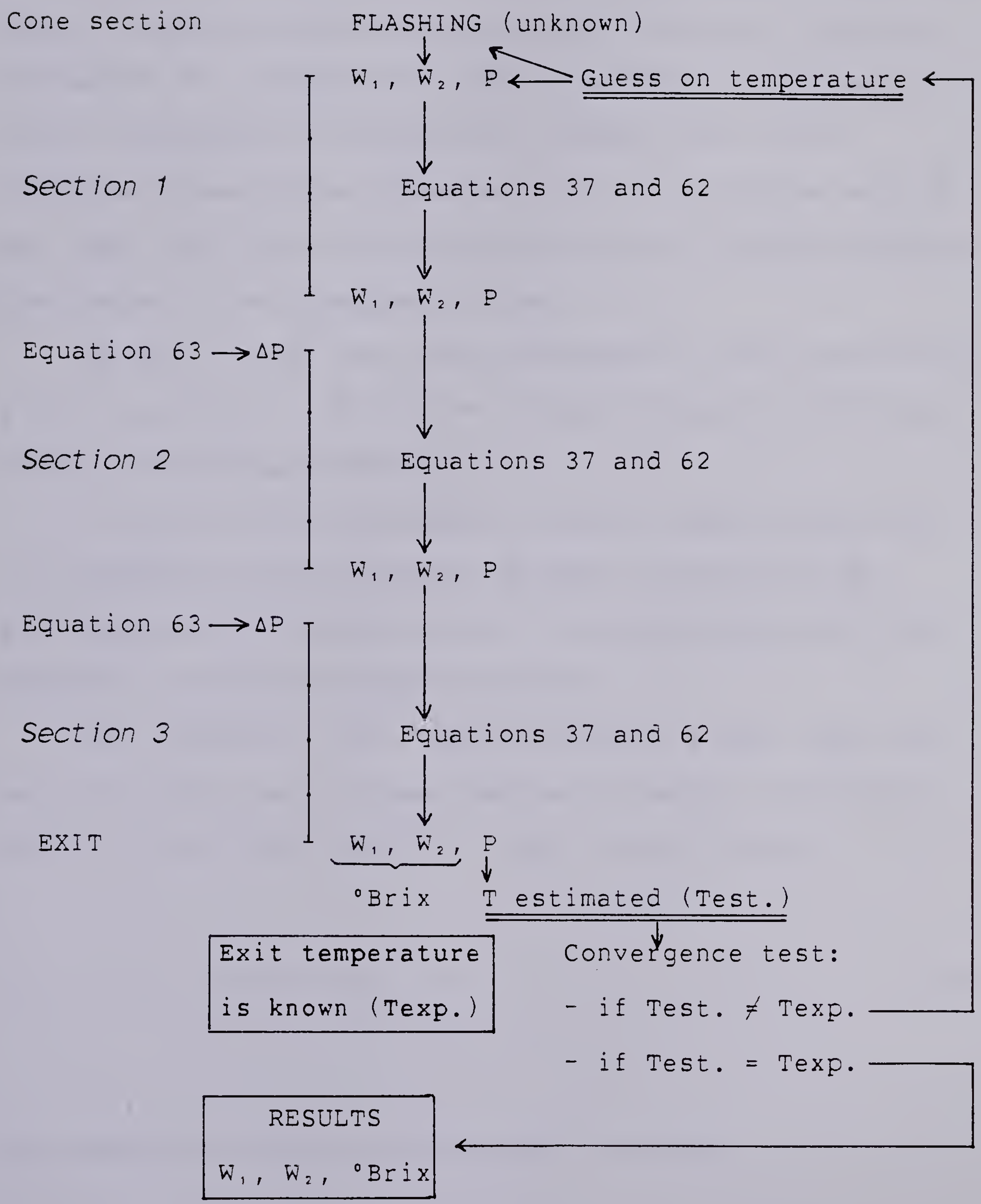
Cone section
FLASHING (unknown)
W_1, W_2, P
Guess on temperature
Section 1
Equations 37 and 62
W_1, W_2, P
Equation 63 → ΔP
Section 2
Equations 37 and 62
W_1, W_2, P
Equation 63 → ΔP
Section 3
Equations 37 and 62
EXIT
W_1, W_2, P
°Brix
T estimated (Test.)
Exit temperature is known (Texp.)
Convergence test:
- if Test. ≠ Texp.
- if Test. = Texp.
RESULTS
W_1, W_2, °Brix

2. Evaluation of the heat transfer coefficient.

When the model was set up for the single tube glass evaporator, an overall heat transfer coefficient between the steam outside the tube and the vapor inside the tube was evaluated. The resistance to heat transfer is composed of three resistances in series: one through the film of condensed steam on the steam side, one through the wall of the tube itself and one through the film of liquid climbing the inside of the evaporator tube.

We have to use the values obtained for the single tube glass evaporator to determine the heat transfer coefficient of the industrial evaporator.

If we know the thickness of the wall and the material it is made of, the resistance through the wall can be evaluated but the resistances on the steam side and on the film side are not directly available.

The diameter of the tubes being much bigger than the wall thickness, we evaluate the heat transfer coefficient using the flat wall equation, which is as follows:

$$1/U = 1/h_s + \Delta x/k + 1/h_f \tag{64}$$

For the glass single tube evaporator we have:

$$1/U_A = 1/h_s + \Delta x_A/k_A + 1/h_f \tag{65}$$

with $\Delta x_A = 1.53\ 10^{-3}$m and $k_A = 1.163$ W.m^{-1}.K^{-1}

For the stainless steel evaporator we have:

$$1/U_B = 1/h_s + \Delta x_B/k_B + 1/h_f \tag{66}$$

with $\Delta x_B = 1.27\ 10^{-3}$m and $k_B = 15$ W.m^{-1}.K^{-1}

Let us assume that the heat transfer coefficients on the steam side are similar in both case and that the heat transfer through the film is the same for a given void fraction α. Elimination of those two factors between Equations 65 and 66 gives:

$$1/U_B = 1/U_A + \Delta x_B/k_B - \Delta x_A/k_A \tag{67}$$

U_A is known for different values of the void fraction α. (refer to Table 5). Then $1/U_B$ and therefore U_B can be evaluated as a function of α. U_B is given by the following equation:

$$U_B = 2539\ \mathrm{W.m^{-2}.K^{-1}} \quad \text{for } \alpha < 0.619$$
$$U_B = 4657.1 - 3423.7\,\alpha \quad \text{for } 0.619 < \alpha < 1 \qquad (68)$$

The square of the multiple correlation coefficients for the first degree best least squares fit is 0.947.

3. Results.

The program converged after 5 iterations. The values of the concentrate rate, temperature and °Brix at the exit of each section are given in Table 8.

The values for Section 3 correspond to a °Brix of 62.24, which is only 0.4% higher than the experimental 62°Brix.

Looking at the vapor rate difference between the model value and the experimental value, we have an experimental rate of 3917 kg.hr^{-1} and a calculated rate of 3919 kg.hr^{-1}. The difference is only 0.05%.

Section number	Conc.rate (kg.s^{-1})	Vap.rate (kg.s^{-1})	Temp. (°C)	°Brix
1	1.093	0.297	89.54	17.17
2	0.754	0.636	88.97	24.89
3	0.302	1.089	88.50	62.24

Table 8. Computed values for the industrial evaporator.

CONCLUSIONS

The results of this investigation indicate that it is possible to predict and control the performance of a climbing film evaporator, assuming the characteristics of the material to be concentrated are known.

The heat transfer in the lower liquid zone is the easiest to solve because it is controlled by very well known parameters (in this zone the evaporator works like a heat exchanger). It was more difficult to solve the problem for the two-phase flow region where no successful theory was previously developed for this kind of evaporator.

In the boiling zone where flashing occurs, our theory is developed from the equations given by Malnes (1975), who worked on superheated liquids encountered in water cooled nuclear reactors. His study was done for very high pressure conditions in the system, while the present work is done under vacuum conditions, making these equations universal for evaporation in vertical tubes when flashing is present.

This is further confirmed by the ability of the model to predict the performance of a big industrial evaporator.

The model can be used to optimize the performance of a given evaporator by determination of the best parameters (feed temperature, feed rate, vacuum and steam pressure) for the concentration of a product from a given initial concentration to a desired final concentration.

The model can also be very useful for the design of an evaporator to accomplish a specific evaporation during a given process. The thermal properties and the amount of product to be concentrated being given, the model can be adapted to determine the size of the evaporator (number of tubes, number of sections and tube length) to be manufactured.

REFERENCES

ARELLANO GAJARDO, R. Concentration of milk and fruit juices by means of climbing film evaporation. An. Fac. Quinn. Farm. p.111. 1972.

BIRD, R.B., STEWART, W.E., and LIGHTFOOT, E.N. Transport phenomena. John Wiley & Sons. N.Y. 1960.

BRENNAN, J.G., BUTTERS, J.R., COWELL, N.D., and LILLY, A.E.V. Food Engineering Operations. Elsevier Publishing Company Ltd. N.Y. 1969.

CARTER, A.L., and KRAYBILL, R.R. Low pressure evaporation. Chem. Eng. Progr. *62*: 99, 1966.

COULSON, J.M., and METHA, R.R. Heat transfer coefficient in a climbing film evaporator. Trans. Instn. Chem. Engers. *31*: 208, 1953.

COULSON, J.M., and McNELLY, M.J. Heat tranfer in a climbing film evaporator. Part II. Trans. Instn. Chem. Engers. *34*: 247, 1956.

GEL'PERIN, N.I., GUROVICH, B.M., and TAKTAEVA, L.N. Heat transfer to boiling aqueous solutions of some electrolytes in a vertical thermosiphon evaporator. Mater. Vses. Nauchno. Tech. p.17. 1973. From Chem. Abs. *83*: 134095g. 1975.

GUERRIERI, S.A., and TALTY, R.D. A study of heat transfer to organic liquids in single-tube, natural-circulation, vertical-tube boilers. Chem. Eng. Progr. *52*: 69, 1956.

KAO, H.S., MORGAN, C.D., CRAWFORD, M., and JONES, J.B. Stability analysis of film boiling on vertical surfaces as a two-phase flow problem. AIchE Symp. Series. Heat Transfer. Tulsa. *68*: #118, pp. 147-155, 1972.

LAWLER, F.K. Revolutionary plate evaporator. Food Eng. *32*, 60-63, 1960.

LEVY, S. Steam slip: Theoretical prediction from momentum model. ASME J. Heat Transfer. *82*: 113-124, 1960.

LOCKHART, R.W., and MARTINELLI, R.C. Proposed correlation of data for isothermal two-phase, two-component flow in pipes. Chem. Eng. Progr. *45*: 39, 1949.

LONCIN, M., and MERSON, R.L. Food Engineering. Principles and selected applications. Academic Press. N.Y. 1979.

LUNDE, K.E. Heat transfer and pressure drop in two-phase flow. Chem. Eng. Progr. Symp. Series. Heat Transfer. Buffalo. *57*: #32, 104-110, 1961.

MALNES, D. Critical two-phase flow based on non-equilibrium effects. Two-Phase Flow Symp.; ASME Winter Annual Meeting. Houston. Texas. 1975.

MOORE, J. G., and HESLER, W.E. Evaporation of heat sensitive materials. Chem. Eng. Progr. *59*: 87, 1963.

PAPADOPOULOS, A., and SAMUEL, O.C. Making beer without a brewhouse. Food Processing *28*: 150, 1965.

PERRY, J.H. Chemical Engineers' Handbook. 4th Edition. McGraw Hill Chemical Engineering Series. N.Y. 1963.

SCOTT, R. Evaporators and Evaporation. Dairy Industries. *29*: 749, 1964.

SEPHTON, H.H. (Sea water convers. lab., Univ. California, Richmond, Calif.). Upflow vertical tube evaporation of sea water with interface enhancement process development by pilot plant testing. *Desalination 16*. pp.1-13, 1975.

SEPHTON, H.H. Renovation of industrial inorganic waste-water by evaporation with interface enhancement. U.S. Environ. Prot. Agency Off. Res. Dev. EPA-600/2-76-017. p.59. 1976.

SEPHTON, H.H., KING, C.J., KLEIN, G., FONG, H.L., FREEL, C.L., HOROWITZ, S.M., PATERSON, R.R., REVAK, T.T., and VALDESKRIEG, E. Interfacial surface enhancement studies. Saline water conversion research program. U. C. Berkeley. Report No.57. p.22. 1973.

SLADE, F.H. Food processing plant. Vol 1. CRC Press, Cleveland, Ohio, 1967.

TAKEDA, H., HAYAKAWA, T., and FUJITA, S. Vapor hold up and boiling heat transfer coefficient in natural circulation vertical tube evaporator. Heat Transfer. Jap. Res. p.34. 1973.(Eng.)

TURNER, J.M. Ph D. Thesis, Darmouth College, Hanover. N.H. 1966.

WALLIS, G.B. One-dimensional two-phase flow. McGraw-Hill. N.Y. 1969.

WEAST, R.C. Handbook of Chemistry and Physics. 55th Edition, CRC Press. Cleveland Ohio. 1974.

WEBRE, A.L., and ROBINSON, C.S. Evaporation. The Chemical Catalog Company, Inc. N.Y. 1926.

APPENDIX A.

Data.

A. Temperature vs pressure for the vapor phase.

The values of temperature vs pressure as given by Loncin and Merson (1979) were used to derive equation 31. The temperatures were converted to absolute temperatures (K).

The first degree best least square fit of ln(T) vs ln(P) is as follow:

$$\ln(T) = 5.11659 + 0.06978 \ln(p)$$

The square of multiple correlation coefficients is: 0.9992.

After exponentiation we obtain:

$$T = 166.766\ P^{0.06978}$$

B. Latent heat of vaporization.

The values of enthalpies of vaporisation as given by Loncin and Merson (1979) were used after conversion to

absolute temperature.

A first degree best least square fit gives:

$$\lambda = 3135665.7 - 2345.714\ T$$

The square of multiple correlation coefficients is 0.9995.

C. Boiling point rise of sugar solutions.

The molecular elevation of the boiling point as given by Weast (1974) is used. For water it is equal to 0.512°C per g-mol/l. The molecular weight of sucrose is 342.3.

%wt/%wt	g-mol/l	T (°C)
17	0.530	0.27
23	0.736	0.38
33	1.101	0.56
40	1.375	0.70

D. Thermal properties.

The tubes of the industrial evaporator are made of 18 gauge stainless steel.

Loncin and Merson (1979) give a thermal conductivity for stainless steel of 15 $W.m^{-1}.K^{-1}$.

The thickness for 18 gauge U.S. standard plate as given by Weast (1974) is 1.27 10^{-3}m.

Weast gives a value of thermal conductivity for borosilicate pyrex type glass of 1.163 $W.m^{-1}.K^{-1}$.

The thickness of the tube of our evaporator was not directly available. The outside diameter was accessible for measurement. The inside diameter was evaluated by measuring the volume of a given height of water: this volume was divided by the height to obtain the inside cross section which was used to evaluate the inside diameter. The thickness is the difference between the outside radius and the inside radius. It was found to be 1.53 10^{-3}m.

Loncin and Merson (1979) give a value of 2,030 $J.kg^{-1}.K^{-1}$ for the heat capacity of the vapor at 100°C. This is half the value of the specific heat of liquid water at the same temperature. When the concentration of the liquid phase increases, its specific heat decreases. Because the heat absorbed by the liquid and the vapor phases is small compared to the heat of vaporisation, in the computer programs we consider that the specific heat of the liquid is identical to that of water while the specific heat of the vapor is taken as half of this value.

APPENDIX B.

Computer program for the boiling zone.

This computer program evaluates the pressure drop and the local heat transfer coefficient in the boiling zone when boiling occurs all along the tube.

This program is composed of a main program and two subroutines.

```
C           PRESSURE DROP IN THE CLIMBING FILM EVAPORATOR
C           IN THE BOILING ZONE.
      COMMON W1,W2,R1,R2,R,DM2,T
C
C          TO EVALUATE THE PRESSURE DROP, THE VOID FRACTION
C          AND THE LOCAL HEAT TRANSFER COEFFICIENT WHEN
C          FILM BOILING IS PRESENT ALL ALONG THE TUBE.
C
      REAL K1,K2,K3,K4
C
C          K1 TO K4 ARE THE RUNGE KUTTA COEFFICIENTS TO
C          EVALUATE DP/DZ*
C
      READ (1,300)K
300   FORMAT (I2)
      NK=0
3     IF(NK.EQ.K) GO TO 1
      NK=NK+1
      READ (1,100)PS,DM,DM2
C
C          PS=STEAM PRESSURE (PSI), DM=FEED RATE (GR/MIN),
C          DM2=VAPOR RATE AT THE EXIT OF THE EVAPORATOR.
C
100   FORMAT (3E12.5)
      READ (1,110)DPV,X
C
C          DPV=VACUUM READING (CM OF MERCURY),
```

```
C              X=DISTANCE AT WHICH BOILING STARTS: X=0.
C
110   FORMAT (2E12.5)
      R1=1000.
      R=0.015
      DM=DM/60000
      DM2=DM2/60000
      WRITE (6,120)PS,DM,DPV
120   FORMAT (/,5X,'ST. PRESS.=',F5.2,5X,
     *'FLOW RATE=',E12.5,5X,'VAC. READING=',F7.2)
      WRITE (6,130)
130   FORMAT (/,5X,'Z=',15X,'TEMP=',12X,'H.T. COEF.=',6X,
     *'ALPHA=',/)
      PS=(14.7+PS)*6890
      N=20
      Y=(76.-DPV)/100.*13600.*9.81
      Z=X
      ALPHA=0.
      TEMP=166.766*Y**0.06978-273.
      H=(1.-Z)/N
2     W2=DM2*Z
      R2=Y**0.93022/77045.892
      W1=DM-W2
      P=Y
C
C              THE VALUE OF DP/DZ* IS EVALUATE IN
c              SUBROUTINE DPM.
```

```
C             THE LOCAL HEAT TRANSFER COEFFICIENT IS EVALUATED
C             IN SUBROUTINE COEF AFTER COMPLETION OF THE RUNGE
C             KUTTA EVALUATION OF DP/DZ*.
C
      CALL DPM(P,DP,U)
      CALL COEF(Z,PS,P,TEMP,DP,UZ)
      WRITE (6,200)Z,TEMP,UZ,ALPHA
      IF(Z.GT.0.99) GO TO 3
      K1=H*DP
      R2=(Y+K1/2.)**0.93022/77045.892
      T=Z+H/2.
      W2=DM2*T
      W1=DM-W2
      P=Y+K1/2.
      CALL DPM(P,DP,U)
      K2=H*DP
      R2=(Y+K2/2.)**0.93022/77045.892
      P=Y+K2/2.
      CALL DPM(P,DP,U)
      K3=H*DP
      R2=(Y+K3)**0.93022/77045.892
      T=Z+H
      W2=DM2*T
      W1=DM-W2
      P=Y+K3
      CALL DPM(P,DP,U)
      K4=H*DP
```

```
      Y=Y+(K1+2.*K2+2.*K3+K4)/6.
      Z=T
      ALPHA=U
      TEMP=166.766*Y**0.06978-273.
200   FORMAT (4(5X,E12.5))
      GO TO 2
1     CONTINUE
      STOP
      END
```

```
      SUBROUTINE DPM(P,DP,U)
C
C              TO DETERMINE THE PRESSURE DROP DP/DZ* IN THE
C              BOILING ZONE.
C
      COMMON W1,W2,R1,R2,R,DM2,T
      REAL J1,J2
      IF (W2.EQ.0.) GO TO 1
C
C              EVALUATION OF THE VOID FRACTION U BY SOLVING
C              EQUATION 38.
C
      A=3.1416*R**2
      C=1.20736E-05
      A1=3.1**2
      D=9.81*0.03*(R1-R2)
      D=SQRT(D)
      J1=W1/SQRT(R1)/A/D
      J2=W2/SQRT(R2)/A/D
      B1=3.1*(J2+J1-1.)
      C1=-J1
      DELT=B1**2-4.*A1*C1
      X=(-B1+SQRT(DELT))/2./A1
      U=1.-X
      S=W2*R1/W1/R2*(1.-U)/U
      V1=W1/R1/A/(1.-U)
      V2=W2/R2/A/U
```

```
      RO=U*R2*S**2+(1.-U)*R1
      Z=R2*U+R1*(1.-U)
      D=V1**2*RO*U*C/R2/P**0.06978
      D=1.-D
      DMV=DM2
      B=(RO*(R1-S*R2)/S/R1/R2+S-1.)*DMV*V1/A
      B=B+9.81*2.67*Z
      DP=-B/D
      GO TO 2
 1    DP=-9.81*2.67*R1
 2    CONTINUE
      RETURN
      END
```

```
      SUBROUTINE COEF(Z,PS,P,TEMP,DP,UZ)
C
C           TO DETERMINE THE LOCAL HEAT TRANSFER COEFFICIENT
C           IN THE BOILING ZONE (UZ).
C
      COMMON W1,W2,R1,R2,R,DM2,T
      REAL LAM
      CP2=4180
      CP1=2000
      X=TEMP+273.
      LAM=3135665.7-2345.714*X
      DMV=DM2
      A=(W2*CP2+W1*CP1)*0.06978*DP/P**0.93022
      A=A+DMV*LAM/166.766
      B=3.1416*2.*R*2.67*(PS**0.06978-P**0.06978)
      UZ=A/B
      RETURN
      END
```

APPENDIX C.

Computer program for the model.

This program evaluates the performance of the evaporator in mormal use given the inlet conditions.

The main program evaluates the distance at which boiling starts and calls the subroutine VAP which evaluates the pressure and the vapor rate in the boiling zone through two other subroutines: DPM and DVAP.

```
C                 CLIMBING FILM EVAPORATOR PROJECT
C             OPERATION OF THE EVAPORATOR IN NORMAL USE.
C             INPUT: STEAM PRESSURE, VACUUM READING.
C             INPUT: FEED TEMPERATURE, FEED RATE
c             IN GRAMS PER MIN.
C             INPUT: THERMAL DIFFUSIVITY, DENSITY,
c             BOILING POINT RAISE.
C             OUTPUT: DIMENSIONLESS LENGTH WHERE
c             BOILING OCCURS.
C             OUTPUT: VAPOR RATE AT EXIT, VOID FRACTION,
C                     TEMPERATURE
C
      COMMON W1,W2,R1,R2,R,ZB,DW2,Y,Z
      R=0.015
3     WRITE (6,210)
210   FORMAT (/,5X,'STEAM PRESSURE=?     VACUUM READING=?')
      READ (5,110)PS,PV
      WRITE (6,220)
220   FORMAT (5X,'FEED TEMPERATURE=?     FEED RATE=?')
      READ (5,110)TI,DM
110   FORMAT(2E12.5)
      DM=DM/60000
      WRITE (6,230)
230   FORMAT (5X,'T.D.=?      DENSITY=?      B.P.RAISE=?')
      READ (5,130)TD,R1,BPR
130   FORMAT (3E12.5)
      WRITE (6,240)
```

```
240    FORMAT (//)
C
C            CALCULATION OF THE DISTANCE AT WHICH BOILING
C            STARTS (ZB) FROM EQUATIONS ESTABLISHED FOR THE
C            LIQUID ZONE.
C
       REPR=4.*DM/R1/3.1416/0.03/TD
       B=-0.4583+(9444.7+5.217E+06/REPR)/REPR
       C=0.2384+(754.6-1.345E+07/REPR)/REPR
       Z0=13./267.
       A=-B*Z0-C*Z0**2
       PV=(76.-PV)/100.*13600.*9.81
       TV=166.766*PV**0.06978-273.
       TV=TV+BPR
       PS=(14.7+PS)*6890.
       TS=166.766*PS**0.06978-273.
       TAU=(TS-TI)/(TS-TV)
       TAU=ALOG(TAU)
       DELT=B**2+4.*C*(TAU-A)
       ZB=(-B+SQRT(DELT))/2./C
       BOIL=ZB*267.
       WRITE (6,200)TI,DM
       WRITE (6,250)BOIL
200    FORMAT (/,5X,'FEED TEMP=',F6.2,5X,'FEED RATE=',E12.5)
250    FORMAT (/,10X,'BOILING STARTS AT Z=',F7.2)
       IF (ZB.GE.1.) GO TO 1
C
```

```
C           THE PRESSURE AND THE VAPOR RATE IN THE BOILING
C           ZONE ARE CALCULATED IN SUBROUTINE VAP FROM
C           Z*=ZB* TO Z*=1.
C
      CALL VAP(DM,PS,PV,TV,U)
      TEMP=166.766*Y**0.06978-273.
      WRITE (6,300)W2,U,TEMP
300   FORMAT (/,10X,'VAPOR RATE=',E12.5,5X,
     *'ALPHA=',E12.5,5X,'TEMP=',F5.2,/)
      GO TO 2
1     WRITE (6,400)
400   FORMAT (/,3X,'ZB BIGGER THAN ONE, TRY NEW GUESS.',/)
2     WRITE (6,450)
450   FORMAT (5X,'SIGN=? IF SIGN=0.STOP, SIGN=1.CONTINUE',/)
      READ (5,120)SIGN
120   FORMAT (E12.5)
      IF (SIGN.EQ.1.) GO TO 3
      STOP
      END
```

```
      SUBROUTINE VAP(DM,PS,PV,TV,U)
C
C           TO DETERMINE THE PRESSURE AND THE VAPOR RATE IN
C           THE BOILING ZONE USING A DOUBLE RUNGE KUTTA 4TH
C           ORDER METHOD.
C
      COMMON W1,W2,R1,R2,R,ZB,DW2,Y,Z
      REAL K1,K2,K3,K4,L1,L2,L3,L4
C
C           K1 TO K4 ARE THE RUNGE KUTTA COEFFICIENTS TO
C           SOLVE EQUATION 37.
C           L1 TO L4 ARE THE RUNGE KUTTA COEFFICIENTS TO
C           SOLVE EQUATION 62
C
      N=20
      H=(1.-ZB)/N
      Z=ZB
      WV=0.
      Y=PV
3     W2=WV
      P=Y
      W1=DM-W2
      R2=P**0.93022/77045.892
C
C           DP/DZ* IS EVALUATED IN SUBROUTINE DPM
C           DW2/DZ* IS EVALUATED IN SUBROUTINE DVAP
C
```

```
CALL DPM(P,DP,U)
CALL DVAP(PS,P,DP)
K1=H*DP
L1=H*DW2
Z=Z+H/2.
W2=WV+L1/2.
P=Y+K1/2.
R2=P**0.93022/77045.892
W1=DM-W2
CALL DPM(P,DP,U)
CALL DVAP(PS,P,DP)
K2=H*DP
L2=H*DW2
P=Y+K2/2.
W2=WV+L2/2.
R2=P**0.93022/77045.892
W1=DM-W2
CALL DPM(P,DP,U)
CALL DVAP(PS,P,DP)
K3=H*DP
L3=H*DW2
Z=Z+H/2.
P=Y+K3
W2=WV+L3
R2=P**0.93022/77045.892
W1=DM-W2
CALL DPM(P,DP,U)
```

```
      CALL DVAP(PS,P,DP)
      K4=H*DP
      L4=H*DW2
      Y=Y+(K1+2.*K2+2.*K3+K4)/6.
      WV=WV+(L1+2.*L2+2.*L3+L4)/6.
      IF (Z.GE.0.999) GO TO 2
      GO TO 3
2     W2=WV
      RETURN
      END
```

```
      SUBROUTINE DPM(P,DP,U)
C
C           TO EVALUATE DP/DZ*
C
      COMMON W1,W2,R1,R2,R,ZB,DW2,Y,Z
      REAL J1,J2
      IF (W2.EQ.0.) GO TO 1
      A=3.1416*R**2
      C=1.20736E-05
      A1=3.1**2
      D=9.81*0.03*(R1-R2)
      D=SQRT(D)
C
C           DETERMINATION OF THE VOID FRACTION U BY SOLVING
C           EQUATION 38.
C
      J1=W1/SQRT(R1)/A/D
      J2=W2/SQRT(R2)/A/D
      B1=3.1*(J2+J1-1.)
      C1=-J1
      DELT=B1**2-4.*A1*C1
      W=(-B1+SQRT(DELT))/2./A1
      U=1.-W
      S=W2*R1/W1/R2*(1.-U)/U
      V1=W1/R1/A/(1.-U)
      V2=W2/R2/A/U
      RO=U*R2*S**2+(1.-U)*R1
```

```
        X=R2*U+R1*(1.-U)
        D=V1**2*RO*U*C/R2/P**0.06978
        D=1.-D
        B=(RO*(R1-S*R2)/S/R1/R2+S-1.)*DW2*V1/A
        B=B+9.81*2.67*X
        DP=-B/D
        GO TO 2
  1     DP=-9.81*2.67*R1
  2     CONTINUE
        RETURN
        END
```

```
      SUBROUTINE DVAP(PS,P,DP)
C
C           TO DETERMINE DW2/DZ*
C
      COMMON W1,W2,R1,R2,R,ZB,DW2,Y,Z
      REAL LAM
      T=166.766*P**0.06978
      LAM=3135665.7-2345.714*T
      COEF=615.5-Z*(112.-41.55*Z)
C
C           COEF=LOCAL HEAT TRANSFER COEFFICIENT IN THE
C           BOILING ZONE AS DEFINED IN EQUATION 55.
C
      CP=4180.
      A=3.1416*0.03*166.766*2.67
      DW2=A*COEF*(PS**0.06978-P**0.06978)
      DW2=DW2-(W2/2.+W1)*CP*166.766*0.06978/P**0.93022*DP
      DW2=DW2/LAM
      RETURN
      END
```

APPENDIX D.

Computer program for the industrial evaporator.

This program evaluates the performance of the industrial evaporator capable of concentrating 5000 kg/hr of pineapple juice from 13.5°Brix to 62°Brix.

This program is composed of a main program and two subroutines.

```
C     COMPUTER PROGRAM TO EVALUATE THE PERFORMANCE
C     OF THE INDUSTRIAL EVAPORATOR.
C
      COMMON W1,W2,R1,R2,R,DW2,Y,Z,L,U,V1,V2
      REAL K1,K2,K3,K4,L1,L2,L3,L4
      H=1./20.
      R=0.0095
      PS=(14.7+35.)*6890.
C
C     INITIAL GUESS ON THE TEMPERATURE: 88.5 C.
C     DT IS THE TEST FOR CONVERGENCE.
C     NK IS TO SET THE EVAPORATOR SECTION.
C     DMF IS THE AMOUNT OF INITIAL FLASHING.
C
      T=88.5+273.
      DT=0.
9     NK=0
      T=T+DT
      P=(T/166.766)**14.331
      DMF=1.39*4000.*(115.5+273.-T)/2.258E+06
      Y=P
      W2=DMF/66.
      W1=(1.39-DMF)/66.
C
C     EVALUATION OF THE INLET CONDITIONS FOR
C     ONE TUBE IN A GIVEN SECTION.
C     R1 IS THE DENSITY OF THE LIQUID PHASE.
```

```
C     R2 IS THE DENSITY OF THE VAPOR PHASE.
C
      L=2.13
8     NK=NK+1
      IF (NK.EQ.1)GO TO 1
      IF (NK.EQ.2)GO TO 2
      L=2.44
      W1=W1*111/156.
      W2=W2*111./156.
      GO TO 1
2     W1=W1*66./111.
      W2=W2*66./111.
1     DM=W1+W2
      Z=0.
      WV=W2
4     W2=WV
      P=Y
      W1=DM-W2
      WW=13.5*DM/W1
      R1=987.7+4.992*WW
      R2=P**0.93022/77045.892
C
C     THE PRESSURE DROP IN THE GIVEN SECTION
C     IS EVALUATED IN SUBROUTINE DPR.
C     THE RATE OF VAPOR FORMATION IS EVALUATED
C     IN SUBROUTINE DV.
C
```

```
CALL DPR(P,DP)
CALL DV(PS,P,DP)
K1=H*DP
L1=H*DW2
Z=Z+H/2.
W2=WV+L1/2.
P=Y+K1/2.
R2=P**0.93022/77045.892
W1=DM-W2
CALL DPR(P,DP)
CALL DV(PS,P,DP)
K2=H*DP
L2=H*DW2
P=Y+K2/2.
W2=WV+L2/2.
R2=P**0.93022/77045.892
W1=DM-W2
CALL DPR(P,DP)
CALL DV(PS,P,DP)
K3=H*DP
L3=H*DW2
Z=Z+H/2.
P=Y+K3
W2=WV+L3
R2=P**0.93022/77045.892
W1=DM-W2
CALL DPR(P,DP)
```

```
      CALL DV(PS,P,DP)
      K4=H*DP
      L4=H*DW2
      Y=Y+(K1+2.*K2+2.*K3+K4)/6.
      WV=WV+(L1+2.*L2+2.*L3+L4)/6.
      TEMP=166.766*Y**0.06978-273.
C
C     TEST TO KNOW WHEN THE TOP OF THE SECTION
C     IS REACHED (Z*=1).
C
      IF (Z.GE.0.999)GO TO 3
      GO TO 4
3     W2=WV
      W1=DM-W2
C
C     TEST TO KNOW WHICH SECTION WAS EVALUATED.
C
      IF (NK.EQ.2)GO TO 5
      IF (NK.EQ.3)GO TO 6
      VAP=W2*66.
      COND=W1*66.
      DEN=R2*U+(1.-U)*R1
      DP1=0.153*DEN*9.81
      Y=Y-DP1
      GO TO 7
5     VAP=W2*111.
      COND=W1*111.
```

```
      DEN=R2*U+(1.-U)*R1
      DP2=0.153*DEN*9.81
      Y=Y-DP2
      GO TO 7
6     VAP=W2*156.
      COND=W1*156.
C
C     OUTPUT AT THE TOP OF EACH SECTION:
C     SECTION, W1, W2, TEMP., ALPHA.
C
7     WRITE (6,100)NK,COND,VAP,TEMP,U
100   FORMAT (5X,I2,4(10X,E12.5))
      IF (NK.LT.3)GO TO 8
C
C     CONVERGENCE TEST ON THE OUTLET TEMPERATURE.
C
      DT=88.5-TEMP
      TEST=ABS(DT)
      WRITE (6,200)
200   FORMAT (/)
      IF (TEST.GT.0.001) GO TO 9
      STOP
      END
```

```
      SUBROUTINE DPR(P,DP)
C
C     TO EVALUATE DP/DZ* IN ONE TUBE OF
C     A GIVEN SECTION.
C
      COMMON W1,W2,R1,R2,R,DW2,Y,Z,L,U,V1,V2
      REAL J1,J2
      IF (W2.EQ.0.) GO TO 1
      A=3.1416*R**2
      C=1.20736E-05
      A1=3.1**2
      D=9.81*2.*R*(R1-R2)
      D=SQRT(D)
C
C     SOLVING EQUATION 38 TO DETERMINE ALPHA.
C
      J1=W1/SQRT(R1)/A/D
      J2=W2/SQRT(R2)/A/D
      B1=3.1*(J2+J1-1.)
      C1=-J1
      DELT=B1**2-4.*A1*C1
      W=(-B1+SQRT(DELT))/2./A1
      U=1.-W
      S=W2*R1/W1/R2*(1.-U)/U
      V1=W1/R1/A/(1.-U)
      V2=W2/R2/A/U
C
```

```
C     SOLVING EQUATION 37.
C
      RO=U*R2*S**2+(1.-U)*R1
      X=R2*U+R1*(1.-U)
      D=V1**2*RO*U*C/R2/P**0.06978
      D=1.-D
      B=(RO*(R1-S*R2)/S/R1/R2+S-1.)*DW2*V1/A
      B=B+9.81*L*X
      DP=-B/D
      GO TO 2
1     DP=-9.81*L*R1
2     CONTINUE
      RETURN
      END
```

```
      SUBROUTINE DV(PS,P,DP)
C
C     TO EVALUATE DW2/DZ*
C
      COMMON W1,W2,R1,R2,R,DW2,Y,Z,L,U,V1,V2
      REAL LAM
      T=166.766*P**0.06978
      LAM=3135665.7-2345.714*T
      CP=4180.
      A=3.1416*2.*R*166.766*L
C
C     DETERMINATION OF THE HEAT TRANSFER
C     COEFFICIENT (EQUATION 68).
C
      IF (U.GE.0.619) GO TO 1
      COEFF=2539.
      GO TO 2
1     COEFF=4657.1-3423.7*U
2     CONTINUE
C
C     SOLVING EQUATION 62.
C
      DW2=A*COEFF*(PS**0.06978-P**0.06978)
      DW2=DW2-(W2/2.+W1)*CP*166.766*0.06978/P**0.93022*DP
      DW2=DW2/LAM
      RETURN
      END
```

B30313